- High $PM_{2.5}$ levels occurred in autumn and winter though annual air quality improved.
- Among WSI, nitrate grew fastest during severe aerosol pollution periods.
- Industrial emission was closely associated with the deterioration of air quality.
- Among ten types of sources, secondary source contributed most to $PM_{2.5}$.
- Regional transport played a key role in enhancement of $PM_{2.5}$ and chemical species.

Characteristics of fine particulate matter and its sources in an industrialized coastal city, Ningbo, Yangtze River Delta, China

Weifeng Wang[1], Jie Yu[1], Yang Cui[2], Jun He[3], Peng Xue[2], Wan Cao[2], Hongmei Ying[1], Wenkang Gao[2, 4], Yingchao Yan[2], Bo Hu[2, 4], Jinyuan Xin[2, 4], Lili Wang[2, 4], Zirui Liu[2, 4], Yang Sun[2, 4], Dongsheng Ji[2, 4*], Yuesi Wang[2, 4*]

[1] *Environment monitoring center of Ningbo, Ningbo 315012, China*

[2] *State Key Laboratory of Atmospheric Boundary Layer Physics and Atmospheric Chemistry, Institute of Atmospheric Physics, Chinese Academy of Sciences, Beijing 100029, China*

[3]*International Doctoral Innovation Centre, Natural Resources and Environment Research Group, Department of Chemical and Environmental Engineering, University of Nottingham Ningbo China, Ningbo, China*

[4]*Center for Excellence in Regional Atmospheric Environment, Institute of Urban Environment, Chinese Academy of Sciences, Xiamen 361021, China.*

[*]Corresponding author:

E-mail address: jds@mail.iap.ac.cn; wys@dq.cern.ac.cn

Abstract

Chemical information is essential in understanding the characteristics of airborne particles, and effectively controlling airborne particulate matter pollution, but it remains unclear in some regions due to the scarcity of measurement data. In the present study, 92 daily $PM_{2.5}$ (particulate matter with an aerodynamic diameter ≤ 2.5 μm) samples as well as historical observation data of air pollutants were collected in urban Ningbo, one of important industrial cities in the coastal area of the Yangtze River Delta, China in autumn and winter (from Nov. 2014 to Feb. 2015). Various chemical species in $PM_{2.5}$ were determined including water soluble ions, organic and elemental carbon and elements. Positive matrix factorization model, cluster analysis of back trajectories, potential source contribution function (PSCF) model and concentration-weighted trajectory (CWT) model were used for identifying sources, apportioning contributions from each source and tracking potential areas of sources. The results showed the $PM_{2.5}$ concentration has been reducing; nonetheless, the concentrations of $PM_{2.5}$ are still much higher than the World Health Organization guideline with high $PM_{2.5}$ concentrations observed in autumn and winter for the past few years. During the sampling period, the average $PM_{2.5}$ mass concentration was 77 μg/m^3 with the major components of OC, NO_3^-, SO_4^{2-}, NH_4^+ and EC, accounting for 26.0, 18.8, 14.5, 11.8 and 6.4% in the total mass concentration, respectively. When the aerosol pollution got worse during the sampling period, the NO_3^-, SO_4^{2-} and NH_4^+ concentrations increased accordingly and NO_3^- appeared to increase at fastest rate. SO_4^{2-} transported from industrial areas led to slight difference in spatial distribution of SO_4^{2-} in Ningbo. More secondary organic carbon was formed and the enrichment factor values of Cu, Ag, Cd, Sn and Pb increased with the degradation of air quality. Ten types of sources were identified for $PM_{2.5}$ in the autumn and winter of Ningbo, which are metallurgical industry, biomass burning and waste incineration, manufacturing related with Mo, chlor-alkli chemical industry, oil combustion, vehicular emission, secondary source, soil dust, road dust and manufacturing related with Cr, accounting for 9.4, 4.8, 9.4, 7.6, 8.1, 18.7, 27.6, 2, 7.1 and 5.2% of the total sources, respectively. There were five groups of air parcels arriving in Ningbo, of which inland air masses originating from Shandong province were associated with the highest $PM_{2.5}$ concentrations. Despite the slight differences, it was obvious that the north of

Jiangxi, east of Anhui, west of Jiangsu, south of Shandong were identified as major potential sources-areas of SO_4^{2-}, NO_3^-, NH_4^+, Cl^-, OC and EC by both PSCF and CWT models.

Keywords: $PM_{2.5}$; Chemical species; Source apportionment; Yangtze River Delta

1. Introduction

$PM_{2.5}$ (particulate matter with an aerodynamic diameter ≤ 2.5 μm) is one of the most important pollutants. It not only has an adverse effect on air quality, human health and atmospheric visibility but also plays a significant role in global climate and ecosystem cycling (WHO, 2005; Fiore et al., 2012; IPCC AR5, 2014; Seinfeld et al., 2016). With roaring economic development, rapid industrialization and urbanization in recent decades, frequent occurrence of haze events was recorded in the Yangtze River Delta (YRD) and the North China Plain (NCP), which was mainly caused by high concentration of $PM_{2.5}$ (Xu et al., 2012; Yang et al., 2015; Zhao et al., 2011), which has attracted public and scientific attention worldwide. To gain sufficient fundamental knowledge for the improvement of regional air quality necessitates a comprehensive study on characteristics of $PM_{2.5}$ and its sources in a specific region (Cheng et al., 2015). Therefore, a detailed understanding of chemical composition and origins of $PM_{2.5}$ is vital for policy-makers to develop effective air pollution control strategies.

YRD is regarded as one of the regions with the most significant anthropogenic sources for $PM_{2.5}$ in the world. Ningbo, with approximately 7.6 million inhabitants (Zhejiang statistical yearbook 2013), is one of the famous economic and industrial centers of YRD region. In addition, Ningbo is an important coastal city located 220 km south of Shanghai and approximately 150 km southeast of Hangzhou, which is a major exporter of electrical products, textiles, food and industrial tools. Although the annual average $PM_{2.5}$ concentrations decreased from 49 to 39 μg/m^3 in Ningbo in recent five years, the $PM_{2.5}$ concentrations were still far higher than the air quality guideline of World Health Organization (annual mean 10 μg/m^3). In particular, severe $PM_{2.5}$ pollution episode frequently occurred in the seasons of autumn and winter. Thus, there is an urgent need in studying the cause of severe $PM_{2.5}$ pollution episode and developing emission policy controls for effectively reducing haze pollution and $PM_{2.5}$ levels in autumn and winter.

A number of studies were conducted to investigate chemical characteristics and potential sources of $PM_{2.5}$ in Ningbo. By chemical mass balance (CMB) receptor model, Xiao et al. (2012) reported that the most important $PM_{2.5}$ sources, based on samples collected in Ningbo during selected one week sampling period for each season (winter, spring, summer and autumn) in 2010,

84 included suspended dust, fly ash from coal combustion, sulfates, vehicle exhaust, nitrates and
85 secondary organic carbon (SOC), with contributions of 19.9, 14.4, 16.9, 15.2, 9.78 and 8.85%,
86 respectively. In addition, Yu et al. (2015) applied positive matrix factorization (PMF) model on
87 aerosol samples collected in winter of 2012 at five sites in Ningbo to quantify the main $PM_{2.5}$
88 sources. Joint observations of air pollution were carried out in YRD and a heavy haze episode was
89 observed from 28 May to 6 June 2011, during which it was found that up to 37% of $PM_{2.5}$ in
90 Ningbo was contributed by the local biomass burning by Weather Research and Forecasting and
91 Community Multiscale Air Quality (WRF/CMAQ) model simulation (Cheng et al., 2014).
92 Recently, Du et al. (2015) studied seasonal and spatial variations of OC and EC in $PM_{2.5}$ in typical
93 periods of 4 seasons from December 2012 to October 2013 in Ningbo and found OC and EC
94 accounted for 17 and 6% of $PM_{2.5}$, and the average concentrations of SOC in summer and autumn
95 accounted for 42 and 28% of total OC, respectively. Xu et al. (2016) captured a high aerosol
96 pollution episode in Ningbo from December 2012 to January 2013 and the analytical results
97 showed that the stagnant meteorological conditions, long-range transport of air masses from heavy
98 industries and biomass burning from northern China to Ningbo could be taken into account as the
99 main factors for such a severe and long-lasting pollution event. Based on the above literature
100 review, most of the air pollution studies in Ningbo were conducted before 2013 when the Air
101 Pollution Prevention and Control Action Plan (APPCAP) was not issued and executed by Chinese
102 government yet; besides, it is known that the autumn and winter are the seasons in which high
103 pollution events can occur most frequently and severely, however, comprehensive studies on the
104 chemical composition and source analysis of $PM_{2.5}$ in Ningbo during both seasons after 2013 have
105 been rarely reported. Thus, a recent study appears to be essential to evaluate if and how the
106 implementation of the APPCAP since 2013 can affect the aerosol pollution status and its source
107 profiles in Ningbo.
108 Therefore, to fill up the abovementioned research gap, a field sampling of $PM_{2.5}$ was
109 conducted in Ningbo during autumn and winter seasons from Nov. 2014 to Feb. 2015. In this
110 study, the chemical compositions of $PM_{2.5}$ were analyzed and their characteristics were
111 summarized; besides, PMF receptor model, cluster analysis of back trajectories, potential source

contribution function (PSCF) and concentration-weighted trajectory (CWT) models, were applied to estimate the relative contributions of sources and identify potential aerosol pollution source areas. The new findings can not only serve as an up-to-date reference database for future field measurement and modeling work, but also are expected to be beneficial for policy-makers to retrofit air pollution control strategy in this region if necessarily in time.

2. Materials and Methods

2.1 Sampling site

The aerosol sampling was conducted from Nov. 4, 2014 to Feb. 6, 2015 at the rooftop of Environment Monitoring Center of Ningbo (SZ, 121°31'41.11"E, 29°53'0.43"N) (Fig. 1). The sampling site is away from the immediate influence of local pollution sources, such as roadside vehicular exhausts and industrial emissions, which is considered to be representative of air pollution level in urban areas of Ningbo. Besides the study site, $PM_{2.5}$ concentrations were also observed at six other sites including Dongqianhu (site 1, rural site), Longsai (site 2, industrial site), Fenghua (site 3, suburban site), Wenfeng (site 4, background site), Cixi (site 5, urban), Wanli (site 6, urban site) and Beilun (site 7, industrial site) during the sampling period.

2.2. Sample collection

$PM_{2.5}$ samplers (Partisol Model 2025 Sequential Air Sampler, Thermo-fisher Scientific Inc. USA) with BGI Inc. Very Sharp Cut Cyclone impactors were used to simultaneously collect $PM_{2.5}$ for 24 h from 0:00 to 23:00 LT every day at a flow rate of 16.7 L min^{-1}, with Quartz fiber and Teflon filters that are 47 mm in diameter. The quartz fiber filters were pre-fired (4 h at 800 °C) to remove all organic impurities. Filters were conditioned in a dryer (25 °C, 40% RH) for 24 h and then they were weighed before and after sampling using a microbalance with sensitivity ±0.01 mg. After sampling, the exposed filters were stored in a freezer at -20 ^{o}C to minimize losses of volatile components. In addition, hourly measurements were conducted for sulfur dioxide (SO_2), nitrogen dioxide (NO_2), carbon monoxide (CO), ozone (O_3) and $PM_{2.5}$ at multiple sites from 2011 to 2015 in Ningbo, and the detailed information on instruments, calibration and maintenance have been reported by Ji et al. (2012).

2.3 Sample analysis

A quarter of each Teflon filter was extracted using 25 ml of deionized water (Millipore, 18.2 MΩ) in an ultrasonic bath for 30 min. The extract liquid was filtered and subsequently analyzed by Ion Chromatograph (IC) (DIONEX, ICS-90, USA) to determine the concentrations of water-soluble ions (Na^+, NH_4^+, K^+, Mg^{2+}, Ca^{2+}, Cl^-, NO_3^- and SO_4^{2-}). The quartz filter was cut and the concentrations of OC and EC were determined using a thermal/optical carbon aerosol analyzer (DRI Model 2001A, Desert Research Institute, USA).

A quarter of the Teflon filter was digested using a mixture of concentrated HF (0.2 ml), HCl (2 ml) and HNO_3 (6 ml) in the automated sample digestion system DEENA (Thomas Cain Inc., USA). The subsequent analysis of trace elements (Na, Mg, Al, K, Ca, Ti, V, Cr, Mn, Fe, Co, Ni, Cu, Zn, As, Mo, Ag, Cd, Sn, Ba, Tl and Pb) was carried out using an Agilent 7500ce inductively coupled plasma mass spectrometry (ICP-MS) (Agilent Technologies, Santa Clara, CA, USA). The analytical methods or protocols of chemical species in $PM_{2.5}$ have been introduced in the previous study (Tian et al., 2016), in which the detailed information on the instruments (e.g., precision, detection limit, operation, calibration and maintenance) and quality assurance/control could be found.

2.4 Positive Matrix Factorization model

Positive Matrix Factorization (PMF) model, an effective receptor modeling tool, has been worldwide applied for source apportionment in the field of environmental research and administration (Brown et al., 2007; Shi et al., 2016). The description of PMF method has been introduced in details in the supplementary materials. The sampling data and the uncertainty of all species based on method detection limit are input into US EPA's PMF 5.0, and source profiles and source contributions can be acquired. Robust uncertainty estimates and diagnostics are shown to assess the rationality of the results. In this study, 33 types of chemical species (Na, Mg, Al, K, Ca, Ti, V, Cr, Mn, Fe, Co, Ni, Cu, Zn, As, Mo, Ag, Cd, Sn, Ba, Tl, Pb, Na^+, NH_4^+, K^+, Mg^{2+}, Ca^{2+}, Cl^-, F^-, SO_4^{2-}, NO_3^-, OC and EC) can be loaded into PMF 5.0, and the sources of $PM_{2.5}$ will be identified and the mass contributions of each source will be also quantified.

166 **2.5 Air mass back trajectory cluster**

167 Forty eight hours backward trajectories arriving at the sampling site (121°31'41.11"E,
168 29°53'0.43"N) were calculated using the HYSPLIT 4 model issued by National Oceanic and
169 Atmospheric Administration (NOAA) during the sampling period. The arrival level was set at 100
170 m above ground level (a.g.l.) and the 48 h back trajectories were calculated at 0:00, 6:00, 12:00
171 and 20:00 UTC.

172 **2.6 PSCF and CWT model**

173 The potential source areas can be identified using potential source contribution function
174 (PSCF) model, which combines the backward trajectory and a defined value of air pollutant
175 (Nicolas et al., 2011). The study field is divided into small equal grid cells (*ij*). The value of PSCF
176 is expressed as:

177 $$PSCF_{ij} = \frac{m_{ij}}{n_{ij}} \quad (1)$$

178 where *i* and *j* denote the latitude and longitude, respectively, n_{ij} represents the number of endpoints
179 passing through the *ij* cell, and m_{ij} is defined as the number of endpoints in the same cell
180 associated with samples that are higher than the criterion value. The 75th percentile for each
181 chemical species is selected as the criterion value. To reduce the uncertainty in cells, a weighting
182 function $w(n_{ij})$ should be multiplied with a m_{ij}/n_{ij} value when n_{ij} is lower than three times of
183 average number of trajectory endpoints (n_{mean}) in each cell (Dimitriou and Kassomenos et al.,
184 2015; Polissar et al., 2001). The weight potential source contribution function (WPSCF) is
185 described as follows:

186 $$WPSCF_{ij} = \frac{m_{ij}}{n_{ij}} \times W(n_{ij}) \quad (2)$$

187 $$W(n_{ij}) = \begin{cases} 1.00, & 3n_{mean} < n_{ij} \\ 0.70, & 1.5n_{mean} < n_{ij} \le 3n_{mean} \\ 0.40, & n_{mean} < n_{ij} \le 1.5n_{mean} \\ 0.20, & n_{ij} \le n_{mean} \end{cases} \quad (3)$$

188 The concentration-weighted trajectory (CWT) model is used to weight trajectories with
189 related concentrations of air pollutants. The geographical field is divided into cells representing an
190 area of 1.0°×1.0°. The CWT can be calculated as follows:

$$C_{ij} = \frac{\sum_{h=1}^{M} C_h \times \tau_{ijh}}{\sum_{h=1}^{M} \tau_{ijh}} \times W(n_{ij}) \quad (4)$$

where C_{ij} is the mean weight concentration of the back trajectory h in the ij cell; C_h represents $PM_{2.5}$ concentration in the trajectory h through ij cell; t_{ijh} represents the time that trajectory h resides in the ij cell. $W(n_{ij})$ used in CWT is the same as that in PSFC to reduce the uncertainty in cells.

The studied domain is from 20 to 50° N and 110 to 130° E, which includes almost all areas covered by all the air mass transport pathways. Both WPSCF and CWT analyses were calculated using the MeteoInfo software-TrajStat Plugin (Wang et al., 2009), which has been proven useful to identify potential source areas of $PM_{2.5}$ and its chemical species (Wang et al., 2015).

3. Result and Discussion

3.1 Levels of $PM_{2.5}$

The levels of $PM_{2.5}$ in Ningbo from 2011 to 2015 and the measurement data for this study are presented in Fig. 2. As shown in Fig. 2(a), clear monthly variations of $PM_{2.5}$ concentrations were observed and higher values were recorded in November, December and January. The monthly average concentrations were 63 ± 29, 79 ± 22 and 86 ± 43 μg/m^3 in November, December 2014 and January 2015, respectively. Given that the electricity and natural gas are the main power sources for residential heating in urban area of Ningbo in autumn and winter (Ningbo Statistical Yearbook, 2015), the increased consumption of coal burning for power generation during these seasons could contribute more to $PM_{2.5}$ concentration in this region. In addition, regional transport or stagnant meteorological condition also played important roles in the accumulation of $PM_{2.5}$ in autumn and winter. As shown in Fig. S1, in the autumn and winter the precipitation (on average 93.9 mm) and WS (on average 1.5 m/s) were lower than annual average values of the precipitation (139.5 mm) and WS (1.7 m/s), respectively. Lower precipitation and WS were conducive to the accumulation of air pollutants. Besides, prevailing northerly wind, which carried air pollutants in NCP and YRD to the sampling site, resulted in the degradation of air quality in Ningbo in the autumn and winter. The results in Fig. 3 show that $PM_{2.5}$ concentrations at all sampling sites in this study were significantly correlated with each other though they are with different urbanization

gradients. Consequently, it can be inferred that the inland air masses transported from outside had a dominant effect on the $PM_{2.5}$ concentrations so as to reduce the spatial variation due to the geographical closeness of all studied sites within Ningbo. It is also consistent with the findings reported by Li et al. (2017) that the continental air masses could import higher concentration of $PM_{2.5}$ to Ningbo. Further discussion will be shown in section 3.4.

As shown in Fig. 2(b), the consistent variations were found between $PM_{2.5}$ concentrations measured using filter sampling and automatic analyzers. The $PM_{2.5}$ concentrations varied from 23 to 204 μg/m^3 with a mean value of 77 μg/m^3 based on filter sampling method. The number of days exceeding the Chinese Ambient Air Quality Standards (CAAQS) daily limit of 75 μg/m^3 was 42, accounting for 48 % of total number of air pollution days in the whole year (from Nov 2014 to Oct 2015). According to American Ambient Air Quality Standard (AAAQS) and World Health Organization (WHO) guideline, there were 83 and 90 days exceeding the daily $PM_{2.5}$ thresholds of 35 μg/m^3 (AAAQS) and 25 μg/m^3 (WHO) during the sampling peiord, respectively. The annual $PM_{2.5}$ concentrations in Ningbo had reduced very slightly from 46 μg/m^3 in 2014 to 45 μg/m^3 in 2015, which were lower than those observed in Ningbo before executing the Air Pollution Prevention and Control Action Plan (Li et al., 2017a). It suggested that APPCAP come into effect and air quality gradually improved. However, the levels of $PM_{2.5}$ increased comparatively from Nov 2013-Feb 2014 to Nov 2014-Feb 2015, which were close to those observed (81.1 μg/m^3) in winter before executing the Air Pollution Prevention and Control Action Plan (Li et al., 2017a). In addition, note that the annual average concentration from Nov 2014 to Oct 2015 is 3 times the AAAQS $PM_{2.5}$ threshold value of 15 μg/m^3, and 4.5 times the WHO guideline value of 10 μg/m^3 in urban Ningbo.

Compared to $PM_{2.5}$ levels in other key cities of YRD, it can be found that the annual average concentration of $PM_{2.5}$ in Ningbo (from Nov 2014 to Oct 2015) was lower than those in Hangzhou (56 μg/m^3), Nanjing (58 μg/m^3), Wuxi (63 μg/m^3), Suzhou (60 μg/m^3) and Shanghai (53 μg/m^3) (China Statistical Yearbook On Environment, 2015). Besides, the annual average concentration of $PM_{2.5}$ in Ningbo was lower than or similar with those in most coastal cities of China, including Tianjin (76 μg/m^3), Qinhuangdao (48 μg/m^3), Qingdao (53 μg/m^3), Danlian (50 μg/m^3) and

Guangzhou (45 μg/m^3), but higher than those of Zhuhai (33 μg/m^3), Shenzhen (33 μg/m^3), Xiamen (34 μg/m^3) and Fuzhou (33 μg/m^3) (China Statistical Yearbook On Environment, 2015). As shown in Fig. S2, moderate correlations were found between $PM_{2.5}$ and SO_2, NO_2, CO and O_x using regression analysis ($P < 0.001$). It is understandable that these gases may be emitted by the same sources that emit $PM_{2.5}$ and its precursors, or themselves may serve as precursors to secondary $PM_{2.5}$ formation. Variations in this complex ambient mixture are accompanied and affected by variations in an array of meteorological conditions. In general, for the past few years the $PM_{2.5}$ concentration has been reducing; nonetheless, the level of $PM_{2.5}$ is still much higher than the WHO guideline and further control measures should be taken to improve air quality in Ningbo.

3.2 Characteristic of chemical composition in $PM_{2.5}$

3.2.1 The major water soluble ions analysis

Tab. 1 and Fig. 4 present concentrations and variations of chemical composition in $PM_{2.5}$ and aerosol chemical profile at various air quality levels (the categorization of air quality levels based on $PM_{2.5}$ concentration bands and the numbers of days with different air quality levels during the sampling period are shown in Tab. S1.) (Ji et al., 2016). Water soluble ions (WSIs) accounted for 45.2% of $PM_{2.5}$ and the NO_3^-, SO_4^{2-}, NH_4^+ and Cl^- were the major WSIs of $PM_{2.5}$ during the sampling period. The concentrations of major WSIs varied in the following order: $NO_3^- > SO_4^{2-} > NH_4^+ > Cl^-$. NO_3^- concentrations ranged from 2.5 to 42.5 μg/m^3 with an average of 14.5 μg/m^3. When the aerosol pollution got worse during the sampling period, the NO_3^-, SO_4^{2-} and NH_4^+ concentrations increased accordingly and NO_3^- appeared to increase at fastest rate. As reported by previous study (Seinfeld et al., 2016), NO_3^- originated from conversion of gaseous NO_x which could be from power plant, traffic emission, shipping emission, industrial combustion and other processes, etc. Based on emission inventory of air pollutants in Ningbo (Tab. S2), it can be seen power plant, mainly the coal-fired boilers, is the predominant source for NO_x, which deems to play an important role in the formation of NO_3^- in Ningbo according to the velocity and conversion rate of NO_3^- from NO_x (Seinfeld and Pandis, 2016). Besides, the observed results also indicated a strong correlation between NO_3^- and SO_2 during the moderately and heavily polluted periods as shown in Fig. 5. It might be because that secondary inorganic ions such as NO_3^- are generated

through both homogeneous and heterogeneous reactions of gaseous precursors including SO_2 and NO_x (Xu et al., 2017).

SO_4^{2-} concentrations ranged from 3.6 to 25.0 μg/m^3 with an average of 11.2 μg/m^3. SO_4^{2-} contributed the second largest portion of the WSIs after NO_3^-. As discussed above, SO_4^{2-} is mainly formed via conversion of primary gaseous pollutant SO_2 and a small fraction can come from marine source. Considering that there is no strong source of SO_2 in the urban areas of Ningbo and sulfur containing fossil fuels are mainly used in industrial facilities (including coal fired power plants) located far away from downtown area in suburb industrial zones or industrial areas of YRD, SO_4^{2-} might be transported from industrial areas leading to slight difference in spatial distribution of SO_4^{2-} in Ningbo (Fig. S3), which was consistent with the results observed by Li et al. (2017).

Cl^- is considered to be an important ion contributing to the formation of $PM_{2.5}$ in coastal cities (Xu et al., 2017). Cl^- showed the high concentration in this study, which may be attributed to both sea source and anthropogenic emission. As reported by Nenes et al. (1998), sea-salt aerosols act as cloud condensation nuclei with SO_2 oxidation proceeding in the resulting cloud droplet producing H_2SO_4 and HNO_3. The formation of H_2SO_4 and HNO_3 promotes the acidity in the NaCl particles, and can result in the evaporation of HCl and decline in the ratio of Cl to Na less than that in sea salt, leading to Cl-depletion. The positive Cl_{excess} of 2.4±2.2 calculated by Eqs (5) and (6) during this study period suggested that Cl^- was influenced by anthropogenic emission more than Cl-depletion process in particular in this study.

$$Cl_{excess} = Cl_{sample} - Cl_{reference} \quad (5)$$

$$Cl_{reference} = Na_{sample}/(Na/Cl)_{sea} = Na_{sample}/0.556 \quad (6)$$

where Cl_{sample} and $Cl_{reference}$ represent the Cl^- concentration observed in the sample and sea-salt sample, respectively, and Na_{sample} is the Na^+ concentration observed in the sample.

NH_4^+ concentrations ranged from 2.3 to 24.2 μg/m^3 with an average of 9.1 μg/m^3. The correlations between equivalent concentrations of NH_4^+ and the total equivalent concentrations of SO_4^{2-}, NO_3^- and Cl^- are reported in Fig. 6, which were very significant indicating NH_4^+ presented similar variation with SO_4^{2-}, NO_3^- and Cl^- in this study. In addition, the slopes of regression lines

were the same with a value of 0.89 throughout the sampling campaign, good and moderate air quality period and polluted days, showing that NH_4^+ equivalent concentrations were not enough to neutralize the sum of SO_4^{2-}, NO_3^- and Cl^- equivalent concentrations. It suggested that $PM_{2.5}$ is acidic but the acidity of these aerosols did not vary significantly with degradation of air quality. Due to instability of NH_4NO_3 and NH_4Cl and deficient NH_4^+ conditions, the formation of $(NH_4)_2SO_4$ and NH_4HSO_4 is more preferred than that of NH_4NO_3 or NH_4Cl (Meng et al., 2011; Seinfeld et al., 2016). In addition, the acidity of the $PM_{2.5}$ is an important parameter affecting the acidity-dependent heterogeneous chemical processes on the aerosol surfaces like the hydrolysis of N_2O_5, the oxidation of SO_2 and the formation of organic aerosols (Wang et al., 2016).

3.2.2 Carbonaceous species

The average concentrations of OC and EC were 19.0 and 4.9 μg/m^3 during this sampling campaign in Ningbo, accounting for 24.7 and 6.4% of $PM_{2.5}$, respectively. The concentrations of OC ranged from 4.7 to 66.1 μg/m^3 while that of EC was in the range between 1.3 and 12.8 μg/m^3. The average OC/EC ratios ranged from 2.0 to 7.7 with an average of 3.9. As shown in Fig. 7(a), with the degradation of air quality, the ratio of OC/EC increased correspondingly. However, the ratios of OC/EC obviously declined with the enhancement of EC concentrations (Fig. 7(b)). EC is essentially a primary pollutant of incomplete fuel combustion including fossil fuel and biomass, etc. (Andersson et al., 2015) and OC originates from primary anthropogenic sources such as fuel combustion and is also formed via secondary transformation of gaseous precursors (Cao et al., 2007; Wang et al., 2012). The increase in OC/EC ratios with enhancement of air pollution levels suggested a significant effect of secondary organic carbon while the decline in OC/EC ratios with enhancement of atmospheric EC levels indicated high EC concentrations and low OC/EC ratios possibly concurred. Local freshly emitted EC under stagnant atmospheric conditions or that transported from upwind high emission areas could result in high concentrations of EC at study site, which usually corresponded with less secondary formation of OC (Aggarwal et al., 2009). However, due to the dispersion during long-range transport and aging effect under sunlight irradiation (Zhao et al., 2016), EC concentrations decreased and more secondary formation of OC could be expected.

As shown in Figs. 7(c) and 7(d), the significant correlation between OC and SO_4^{2-} but the insignificant correlation between EC and SO_4^{2-} were observed, which confirmed that secondary formation played an important role in the generation of OC and sulfate through homogeneous and/or heterogeneous reactions. In addition, the average ratio of OC/EC was 3.9 in Ningbo in this study, which again supported the strong contribution of SOC to $PM_{2.5}$ in this study, as the ratio of OC/EC greater than 2.0 could be generally applied to identify and evaluate secondary organic aerosols (Chow et al., 1996; Turpin and Huntzicker, 1991).

To further evaluate the contributions of both primary and secondary organic carbon to carbonaceous aerosol, the equations (7) and (8) below are used (Turpin and Huntzicker, 1995):

$$OC_{sec} = OC_{tot} - EC \times (OC/EC)_{min} \quad (7)$$

$$OC_{pri} = EC \times (OC/EC)_{min} \quad (8)$$

where OC_{sec} is secondary OC, OC_{tot} is total OC, OC_{pri} is primary OC, and $(OC/EC)_{min}$ is the minimum ratio of OC/EC, which could replace the ratio of OC/EC in the primary aerosol. The $(OC/EC)_{min}$ in the lowest 10% OC/EC ratios would be a reasonable estimate of the primary emissions in this study (Lim et al., 2002; Wu et al., 2016). The results showed that the fraction of SOC in total carbon (TC) was 43.0%, and SOC accounted for 41.3, 39.4, 38.7, 52.4 and 52.3% of TC when air quality were excellent, good, lightly polluted, moderately polluted and heavily polluted, respectively. The higher percentage (52.4 and 52.3%) of SOC during the moderately and heavily polluted periods might be related to rapid transformation of the SOC precursors, i.e., VOCs (Cao et al., 2005).

3.2.3 Elemental profile

As shown in Tab. 1, twenty-two elements were analyzed in the aerosol samples, including Na, Mg, Al, K, Ca, Ti, V, Cr, Mn, Fe, Co, Ni, Cu, Zn, As, Mo, Ag, Cd, Sn, Ba, Tl and Pb, the total concentration of elements accounted for only 5.5% of $PM_{2.5}$ during the sampling period with average concentration of all elements of 4.2 μg/m^3. As shown in Tab. S3, significant positive correlations between $PM_{2.5}$ and Na, K, Mn, Fe, Co, Cu, As, Mo, Ag, Cd, Sn, Ba as well as Pb (2-tailed, $P<0.001$) were found, indicating that the above-mentioned elements increased with enhancement of $PM_{2.5}$ concentrations. The concentration of K, Na, Al, Ca, Fe, Zn and Mg

accounted for 93% of the total concentration of all measured elements in this study. From the literature (Song et al., 2001), K, Al, Ca and Fe were associated with crustal sources; besides, Fe and K originated from industrial emission and biomass burning, respectively. Significant correlations between Fe and Cd (Tab. S3) as well as K and EC (Fig. S4) supported the results, which showed Cd came from metallic smelting and biomass burning emitted EC and K simultaneously. The mass concentrations of Ni (0.010±0.005 μg/m^3) and V (0.006±0.005 μg/m^3) in this study were comparable to those observed in Ji'nan, China (Gu et al., 2014) and significant correlation between Ni and V might imply that Ni and V originated from the same source, which was consistent with the finding in previous studies that shipping emission was characteristic of high Ni and V concentrations (Tao et al., 2017). The average concentrations of Mn, Cu, Zn, Cr, Co, Cd, and Pb were 0.057±0.037, 0.027±0.014, 0.376±0.229, 0.029±0.013, 0.0004±0.0002, 0.002±0.001 and 0.091±0.055 μg/m^3, respectively, which deemed to be mainly from metal smelting (Amato et al., 2012; Liu et al., 2016). V, Cr, Ni, Co, Sr and Cd showed no obvious variations, probably related to various industrial activities (Yang et al., 2013; Yao et al., 2016).

Enrichment factor (*EF*) has been widely applied to evaluate the enrichment degrees of elements using the equation (9):

$$EF = (X/X_{Ref})_{environment}/(X/X_{Ref})_{background} \quad (9)$$

where X is element in the studied environment and X_{Ref} is the reference element (Huang et al., 2012). Al is used as the reference element in this study (Liu et al., 2017; Wang et al., 2016; Zhang et al., 2015). $(X/X_{Ref})_{background}$ was obtained based on concentrations in topsoil in China (Wei et al., 1991). The *EF* values of Ti, Mg, Fe, Co, Ba, Ca, K, Na, V, Mn, Ni, Cr, As, Mo, Cu, Tl, Pb, Ag, Sn, Zn and Cd ranged from 1.0 to 2, 892.6 during the sampling period. The *EF* values of Ti, Mg, Fe, Co, Ba, Ca, K, Na were lower than 10, suggesting that they mainly originated from natural sources while those of V, Mn, Ni, Cr, As, Mo, Cu, Tl, Pb, Ag, Sn, Zn and Cd were higher than 10, indicating that these elements were closely related to anthropogenic activities (Wang et al., 2013). Mg and Na could be attributed to sea salt while Ti, Fe, Co, Ba, Ca and K were bound up with crustal sources. The *EF* value of Cd varied from 184.4 to 8,605.8, which were associated with anthropogenic emission i.e., intensive industrial processes (Wang et al., 2013). Note that with the

deterioration of air quality the *EF* values of Cu, Ag, Cd, Sn and Pb increased accordingly, which indicated enhancement in effect of their anthropogenic emission on the worse local air quality.

3.3. Source apportionment

To avoid repeated calculation, K, Na, Ca and Mg measured by ICP-MS were utilized instead of those ions analyzed by IC for the source analysis by PMF modeling. In final, 30 variables were input into the PMF model including $PM_{2.5}$, F^-, Cl^-, NO_3^-, SO_4^{2-}, NH_4^+, OC, EC, Na, Mg, Al, K, Ca, Ti, V, Cr, Mn, Fe, Co, Cu, Ni, Ag, Tl, Zn, As, Mo, Ba, Cd, Sn and Pb. Of all the variables, $PM_{2.5}$ was considered as the total variable. After initial examination of PMF model, Ni, Ag and Tl were eliminated from the model due to the poor match between the modeled and measured values. The measured concentrations of chemical species input into the PMF model accounted for 80.2% of the total $PM_{2.5}$. 5-13 factors were attempted in the PMF model operation (Tab. S4). After optimization, 10 factors were determined as input parameters by Error Estimation (EE) diagnostics analysis and the most reasonable results were acquired. The regression line between the $PM_{2.5}$ concentration (y) produced by the PMF modeling and that measured in this study (x) could be expressed as $y = 0.89x + 3.37$ ($r^2 = 0.86$). $Q_{(Robust)}/Q_{(True)}$ of 0.93 also indicated that ten factors could be an optimal solution. The spectrum of different sources for $PM_{2.5}$ in this study estimated by PMF model was shown in Fig. 8. Besides, the contribution of each source by weight percentage was presented in Fig. 9 and time series of the contribution from different sources was shown in Fig. S5.

The first source category of $PM_{2.5}$ was metallurgical industry, accounting for 9.4% of $PM_{2.5}$. This source was characterized by high loading of Mn and Zn and moderate loading of Fe, Co and Cu, which is consistent with findings in previous studies (Kim et al., 2003; Song et al., 2006). As documented by economic census conducted by Ningbo statistics bureau (http://english.nbtjj.gov.cn), there were approximately 5,082 enterprises related to metal smelting and processing.

The source factor 2, contributing 4.8 % to $PM_{2.5}$, was characteristic of high contribution of K and moderate loading of Pb, As, Cd, Cu, OC and EC. It was reported in previous studies that high contribution of K and Pb could be from biomass burning and waste incineration (Huang et al., 2014; Yuan et al. 2006).

414 The third source factor had high proportion of Mo and the moderate loadings of Co, Cu, Fe
415 and Zn, which could be identified as industrial processes related with Mo (Tao et al., 2014), and
416 this factor accounted for 9.4% of $PM_{2.5}$. This might be supported by such a fact that there are
417 plenty of enterprises related to Mo production and manufacturing according to the field
418 investigation in Ningbo (http://english.nbtjj.gov.cn).
419 Factor 4 had a significant contribution of Cl^-, accounting for 7.6% of $PM_{2.5}$. In addition to
420 marine source (seawater), coal combustion and chlor-alkli chemical industry could be identified as
421 the main source for Cl^- in this study (Xu et al., 2017; Liu et al., 2017).
422 The fifth factor had a highest loading of V with an average contribution of 8.1% to $PM_{2.5,}$
423 which was the indicator of heavy oil combustion (Vallius et al., 2003). Heavy oil is normally used
424 for cargo ships and diesel vehicles etc. (Vallius et al., 2003; Yao et al., 2016; Tao et al., 2017).
425 The sixth type of source was characterized by EC and OC and also contained high loadings
426 of SO_4^{2-}, NH_4^+ and Ca. The OC and EC are major pollutants from gasoline and diesel combustion
427 (Zhang et al., 2017; Yao et al., 2016). Hence, vehicle exhaust could be identified for this factor
428 and contributed 18.7% to $PM_{2.5}$. The sampling site was located in the downtown area of Ningbo,
429 densely populated and heavily affected by nearby traffic activities.
430 Factor 7 was highly loaded with SO_4^{2-}, NO_3^- and NH_4^+, representative of contribution by
431 secondary inorganic aerosols (Gao et al., 2016; Zhang et al., 2017). A number of studies suggested
432 that NO_3^-, SO_4^{2-} and NH_4^+ were mainly stemmed from the conversion processes of gaseous
433 precursors to particle (Liu et al., 2015; Tao et al., 2013; Wang et al., 2006). This factor accounted
434 for 27.6% of $PM_{2.5}$, possessing the highest contribution to these fine aerosols, indicating its
435 important roles in worsening the air quality and visibility reduction in this region.
436 The eighth category of pollution sources was characterized by elements including the Mg, Al,
437 Ca and Ti, which are of crustal source or soil dust, contributing an average of 2% of $PM_{2.5}$. This
438 was consistent with findings in a previous study conducted in urban Ningbo (Yu et al., 2015).
439 The ninth factor had high abundance of Al and V, indicating a strong contribution from road
440 dust accounting for 7.1% of $PM_{2.5}$ (Li et al., 2016). As mentioned above, the population of

automobiles was large and traffic in downtown area was heavy, hence it might be understandable that road dust could be a more important source than soil dust for $PM_{2.5}$ in this study.

The tenth factor was associated with industrial emission, characteristic of a significant loading of Cr. In addition, a certain amount of Mn, Zn and Al was also observed in this factor. This factor contributed 5.2% to $PM_{2.5}$.

Based on the above analysis, it is found that the contribution of the secondary inorganic aerosol was the largest source and the control of gaseous precursor like SO_2, NO_x and NH_3, etc. should be further strengthened. Vehicular exhaust was the second largest source, which suggested that advanced technology needs to be implemented to more effectively control traffic emission. Manufacturing and other industrial processes in relation to Mo, Cr and Cl^- contributed 22.2% to $PM_{2.5}$. In addition, it is also clear that the road and soil dust emission should be further suppressed in near future.

3.4. Source analysis based on backward trajectories, WPSCF and CWT

Figs. 10, 11 and 12 showed the association of the backward trajectories with $PM_{2.5}$, and potential sources-areas of NO_3^-, SO_4^{2-}, NH_4^+, Cl^-, OC, EC and $PM_{2.5}$, during the sampling period. In terms of directions and traveled regions, major trajectories were divided into five groups by cluster analysis: (1), (2), (3), (4) and (5), accounting for 31.4, 14.5, 27.1, 12.2 and 14.0% of the total trajectories, respectively. The $PM_{2.5}$ concentrations in every group were shown in Tab. S5. Trajectory (1) stemmed from Shandong province, which clearly represented inland air masses. The highest $PM_{2.5}$ concentrations were associated with this group of trajectories. Trajectory (2) began in Liaoning province, passed through ocean before arriving at Ningbo. Trajectory (3) was originated from the East China Sea with relatively shorter pathways, which were bound up with the lowest $PM_{2.5}$ concentrations. Trajectory (4) originated from Mongolia, across over Inner Mongolia, Hebei province, the Bohai Sea, Shandong province and the East China Sea before arriving at the sampling site, which showed the extremely long transport pathway. Trajectory (5) was originated from Anhui province, across over the border of Jiangsu and Zhejiang provinces before arriving at Ningbo, which showed the extremely shorter transport pathway, associated with higher $PM_{2.5}$ concentrations.

As shown in Figs. 11 and 12, the most areas of Jiangsu province, eastern areas of Anhui province, south of Shandong province and northeastern areas of Zhejiang province were identified as major potential sources-areas of $PM_{2.5}$ as well as NO_3^-, SO_4^{2-}, NH_4^+, Cl^-, OC and EC based on WPSCF and CWT models. However, slight difference in potential source areas of NO_3^-, SO_4^{2-}, NH_4^+, Cl^-, OC and EC was found. For example, high potential source areas and transport pathways of NO_3^-, SO_4^{2-}, Cl^-, OC and EC were mainly located in the north and northwest of Ningbo including areas of Jiangsu province, the north of Zhejiang province, the south of Shandong province and Jiujiang city in Jiangxi province, where the largest coal-fired thermal power plant in Jiangxi province was located. NH_4^+ shared the similar source regions with NO_3^-, SO_4^{2-}, Cl^-, OC and EC but had less high potential source areas across the abovementioned regions. The possible reason for this was that the source of NH_4^+ is different from those of NO_3^-, SO_4^{2-}, Cl^-, OC and EC. NH_4^+ originated from the transformation of NH_3 (Seinfeld et al., 2016), which mainly come from agricultural activities (Wu et al., 2016). In addition, the partial areas of Yellow Sea and East China Sea were identified as high potential sources-areas of Cl^-. Note that NO_3^-, SO_4^{2-}, Cl^-, OC and EC had obvious high potential source areas across inland regions including Yangzhou-Zhenjiang-Changzhou-Wuxi-Suzhou-Jiaxing cities. Considering that many cities located along this pathway are industrial cities, such as Yangzhou, Zhenjiang, Changzhou, Wuxi, Suzhou and Jiaxing, regional transport from these areas would have potentially high impact on the formation of severe pollution. In addition, regional transport from Taizhou industrial regions in Zhejiang province, which is located in the south of Ningbo, might play an important role in the high concentrations of NO_3^-, SO_4^{2-}, Cl^-, OC and EC. Such a pollution band agrees well with a previous study (Li et al., 2017b).

4. Conclusion

An intensive experiment was conducted to study the characteristics of $PM_{2.5}$ and its sources in Ningbo, an important industrial city in the coastal area of the Yangtze River Delta, China in both autumn and winter seasons. The major gaseous pollutants, $PM_{2.5}$ and its chemical compositions were concurrently measured. Based on PMF, PSCF and CWT models, sources of

496 $PM_{2.5}$ were identified, and sources areas of $PM_{2.5}$ and its chemical species were investigated. The
497 conclusions were summarized as below:

498 The annual average $PM_{2.5}$ concentrations declined in past few years, but were still far higher
499 than the WHO guideline. In particular, the $PM_{2.5}$ pollution episodes frequently occurred in autumn
500 and winter, when further control measures should be taken to improve air quality in Ningbo. It
501 appears that regional transport played important roles in high aerosol pollution in both seasons.

502 The water-soluble ions, carbonaceous species and elements contributed 48.7±14.8%,
503 29.9±8.0% and 5.5±9.0% to $PM_{2.5}$, respectively. Based on the emission inventory and the
504 relationship between NO_3^- and SO_2, industrial emission played an important role in formation of
505 NO_3^-. Controlling NO_x from industrial emission will be helpful for reducing $PM_{2.5}$ level in
506 Ningbo. With the degradation of air quality, the ratio of OC/EC increased correspondingly and
507 suggested that secondary organic aerosol contributed significantly to OC. In addition, industrial
508 emissions played a more important role when air quality became more polluted based on *EF*
509 values.

510 Ten types of sources were determined via PMF model analysis based on the EE diagnostics.
511 Secondary source was the highest contributor to $PM_{2.5}$ in Ningbo for the whole study period, and
512 followed by vehicular emission, metallurgical industry, manufacturing related with Mo, oil
513 combustion, chlor-alkli chemical industry, road dust, manufacturing related with Cr, biomass
514 burning and waste incineration and soil dust, respectively.

515 The most areas of Jiangsu province, eastern areas of Anhui province, south of Shandong
516 province and northeastern areas of Zhejiang province were identified as major potential sources-
517 areas of $PM_{2.5}$ as well as NO_3^-, SO_4^{2-}, NH_4^+, Cl^-, OC and EC by WPSCF and CWT models. In
518 addition, the partial areas of Yellow Sea and East China Sea were identified as high potential
519 sources-areas of Cl^-. Due to the transboundary transport effect, joint pollution prevention and
520 control measures need to be strengthened to improve the air quality in this region.

521 **Acknowledgment**

522 This work is supported by the National Key Research and Development Program of China
523 (2016YFC0202701), Ningbo Science and Technology Foundation (16YFZCSF00260) and Beijing

Municipal Science and Technology Project (D171100001517003). The authors also gratefully acknowledge Ningbo Environmental Monitoring Center for supporting in the monitoring campaign.

Reference

Aggarwal, S. G., Kawamura, K., 2009. Carbonaceous and inorganic composition in long-range transported aerosols over northern Japan: Implication for aging of water-soluble organic fraction. Atmospheric Environment 43(16), 2532-2540.

Amato, F., Hopke, P. K., 2012. Source apportionment of the ambient $PM_{2.5}$ across St. Louis using constrained positive matrix factorization. Atmospheric Environment 46, 329-337.

Bao, C., Chai, P., Lin, H., Zhang, Z., Ye, Z., Gu, M., Lu, H., Shen, P., Jin, M., Wang, J., Chen, K., 2016. Association of $PM_{2.5}$ pollution with the pattern of human activity: A case study of a developed city in eastern China. Journal of the Air & Waste Management Association 66, 1202-1213.

Brown, S. G., Frankel, A., Hafner, H. R., 2007. Source apportionment of VOCs in the Los Angeles area using positive matrix factorization. Atmospheric Environment 41, 227-237.

Cao, J. J., Wu, F., Chow, J. C., Lee, S. C., 2005. Characterization and source apportionment of atmospheric organic and elemental carbon during fall and winter of 2003 in Xi'an, China. Atmospheric Chemistry & Physics *5*(11), 3127-3137.

Cheng, Z., Wang, S., Fu, X., Watson, J.G., Jiang, J., Fu, Q., Chen, C., Xu, B., Yu, J., Chow, J.C., Hao, J., 2014. Impact of biomass burning on haze pollution in the Yangtze River delta, China: a case study in summer 2011. Atmospheric Chemistry and Physics 14, 4573-4585.

China Statistical Yearbook On Environment, 2015. National Bureau of Statistics of China. ISBN 978-7-5037-8090-5.

Dimitriou, K., Kassomenos, P., 2015. Three year study of tropospheric ozone with back trajectories at a metropolitan and a medium scale urban area in Greece. Science of the Total Environment 502, 493-501.

Du, B. H., Huang, X. F., He, L. Y., Hu, M., Wang, C., Ren, Y. C., Ying, H. M., Zhou, J., Wang, W. F., Xu, D. D., 2015. Seasonal and Spatial Variations of Carbon Fractions in $PM_{2.5}$ in Ningbo and the Estimation of Secondary Organic Carbon. Environmental Science(China) 36, 3128-3134.

Fiore, A. M., Naik, V., Spracklen, D. V., Steiner, A., Unger, N., Prather, M., Bergmann, D., Cameron-Smith, P. J., Cionni, I., Collins, W. J., Dalsøren, S., Eyring, V., Folberth, G. A., Ginoux, P., Horowitz, L.W., Josse, B., Lamarque, J.-F., MacKenzie, I. A., Nagashima, T., O'Connor, F. M., Righi, M., Rumbold, S. T., Shindell, D. T., Skeie, R. B., Sudo, K., Szopa, S., Takemura, T., Zeng, G., 2012. Global air quality and climate, Chem. Soc. Rev. 41, 6663.

Gao, J., Peng, X., Chen, G., Xu, J., Shi, G. L., Zhang, Y. C., Feng, Y. C. 2016. Insights into the chemical characterization and sources of $PM_{2.5}$ in Beijing at a 1-h time resolution. Science of the Total Environment 542, 162-171.

Gu, J., Du, S., Han, D., Hou, L., Yi, J., Xu, J., et al. 2014. Major chemical compositions, possible sources, and mass closure analysis of $PM_{2.5}$, in Jinan, china. Air Quality Atmosphere & Health 7(3), 251-262.

Huang, K., Zhuang, G., Lin, Y., Wang, Q., Fu, J.S., Zhang, R., Li, J., Deng, C., Fu, Q., 2012. Impact of anthropogenic emission on air quality over a megacity–revealed from an intensive atmospheric campaign during the Chinese Spring Festival. Atmospheric Chemistry and Physics 12, 11631-11645.

IPCC AR5, 2014. Climate Change 2014: The Physical Science Basis. Contribution of Working Group I to the Fifth Assessment Report of the Intergovernmental Panel on Climate; IPCC; Cambridge University Press, Cambridge.

Ji, D. S., Zhang, J. K., He, J., Wang, X. J., Pang, B., Liu, Z. R., Wang, L. L., Wang, Y. S., 2016. Characteristics of atmospheric organic and elemental carbon aerosols in urban Beijing, China. Atmospheric Environment 125, 293-306.

Ji, D., Wang, Y., Wang, L., Chen, L., Hu, B., Tang, G., Xin, J., Song, T., Wen, T., Sun, Y., 2012. Analysis of heavy pollution episodes in selected cities of northern China. Atmospheric Environment 50, 338-348.

Li, H., Wang, Q., Yang, M., Li, F., Wang, J., Sun, Y., et al., 2016. Chemical characterization and source apportionment of $PM_{2.5}$, aerosols in a megacity of southeast china. Atmospheric Research 181, 288-299.

Li, M. R., Hu, M., Du, B. H., Guo, Q. F., Tan, T. Y., Zheng, J., Huang X. F., He, L. Y., Guo, S., 2017a. Temporal and spatial distribution of $PM_{2.5}$ chemical composition in a coastal city of Southeast China. Science of The Total Environment 605, 337-346.

Li, S. X., Zou B., Liu X. Q., Fan X., 2017b. Pollution Status and Spatial-Temporal Variations of $PM_{2.5}$ in China during 2013-2015. Research of Environmental Sciences, 30(5):678-687.

Lim, H. J. and Turpin, B. J., 2002. Origins of primary and secondary organic aerosol in Atlanta: results of time-resolved measurements during the Atlanta supersite experiment. Environmental Science & Technology, 36, 4489–4496.

Liu, B. S., Wu, J. H., Zhang, J. Y., Wang, L., Yang, J. M., Liang, D. N., Dai, Q. L., Bi, X. H., Feng, Y. C., Zhang, Y. F., Zhang, Q. X., 2017. Characterization and source apportionment of $PM_{2.5}$ based on error estimation from EPA PMF5.0 model at a medium city in China. Environmental Pollution, *222*, 10-22.

Liu, B., Song, N., Dai, Q., Mei, R., Sui, B., Bi, X., Feng, Y., 2016. Chemical composition and source apportionment of ambient $PM_{2.5}$ during the non-heating period in Taian, China. Atmospheric Research, 170, 23-33.

Liu, X. G., Li, J., Qu, Y., Han, T., Hou, L., Gu, J., Chen, C., Yang, Y., Liu, X., Yang, T., Zhang, Y., Tian, H., Hu, M., 2013. Formation and evolution mechanism of regional haze: a case study in the megacity Beijing, China. Atmospheric Chemistry and Physics 13, 4501.

Liu, Z. R., Hu, B., Zhang, J., Yu, Y. C., Wang, Y. S., 2016. Characteristics of aerosol size distributions and chemical compositions during wintertime pollution episodes in Beijing. Atmospheric Research, 168, 1-12.

McCarthy, M. C., Aklilu, Y. -A., Brown, S. G., Lyder, D. A., 2013. Source apportionment of volatile organic compounds measured in Edmonton, Alberta. Atmospheric Environment 81, 504-516.

Nenes, A., Pandis, S.N., Pilinis, C., 1998. ISORROPIA: A New Thermodynamic Equilibrium Model for Multiphase Multicomponent Inorganic Aerosols. Aquatic Geochemistry 4, 123-152.

Polissar, A. V., Hopke, P. K., Poirot, R. L., 2001. Atmospheric Aerosol over Vermont: Chemical Composition and Sources. Environmental Science & Technology 35, 4604-4621.

Seinfeld, J. H., Pandis, S. N., 2016. Atmospheric Chemistry and Physics: From Air Pollution to Climate Change. John Wiley & Sons.

Shi, G. L., Chen, H., Tian, Y. Z., Song, D. L., Zhou, L. D., Chen, F., Yu, H. F., Feng, Y. C., 2016. Effect of uncertainty on source contributions from the positive matrix factorization model for a source apportionment study. Aerosol and Air Quality Research, 16(7), 1665-1674.

Song, X. H., Polissar, A. V., Hopke, P. K., 2001. Sources of fine particle composition in the northeastern US. Atmospheric Environment 35, 5277-5286.

Tao, J., Gao, J., Zhang, L., Zhang, R., Che, H., & Zhang, Z., et al. 2014. $PM_{2.5}$ pollution in a megacity of southwest china: source apportionment and implication. Atmospheric Chemistry & Physics, 14(4), 8679–8699.

Tao, J., Zhang, L., Cao, J., Zhong, L., Chen, D., Yang, Y., et al., 2017. Source apportionment of $PM_{2.5}$ at urban and suburban areas of the Pearl River Delta region, south China-With emphasis on ship emissions. Science of The Total Environment, 574, 1559-1570.

Tian, S. L., Pan, Y. P., Wang, Y. S., 2016. Size-resolved source apportionment of particulate matter in urban Beijing during haze and non-haze episodes. Atmospheric Chemistry and Physics 16, 1-19.

Vallius, M., Lanki, T., Tiittanen, P., Koistinen, K., Ruuskanen, J., Pekkanen, J., 2003. Source apportionment of urban ambient $PM_{2.5}$ in two successive measurement campaigns in Helsinki, Finland. Atmospheric Environment 37, 615-623.

Wang G, Zhang R, Gomez M E, et al., 2016. Persistent sulfate formation from London Fog to Chinese haze. Proceedings of the National Academy of Sciences, 113(48), 13630-13635.

Wang, J., Hu, Z., Chen, Y., Chen, Z., Xu, S., 2013. Contamination characteristics and possible sources of PM_{10} and $PM_{2.5}$ in different functional areas of Shanghai, China. Atmospheric Environment 68, 221-229.

Wang, P., Cao, J. J., Tie, X. X., Wang, G. H., Li, G. H., Hu, T. F., Wu, Y. T., Xu, Y. S., Xu, G. D., Zhao, Y. Z., Ding, W. C., Liu, H. K., Huang, R. J., Zhan, C. L., 2015. Impact of Meteorological Parameters and Gaseous Pollutants on $PM_{2.5}$ and PM_{10} Mass Concentrations during 2010 in Xi'an, China. Aerosol and Air Quality Research 15, 1844-1854.

Wang, Y. Q., Zhang, X. Y., Draxler, R. R., 2009. TrajStat: GIS-based software that uses various trajectory statistical analysis methods to identify potential sources from long-term air pollution measurement data. Environmental Modelling & Software, 24(8), 938-939.

Wang, Y., Jia, C., Tao, J., Zhang, L., Liang, X., Ma, J., Gao, H., Huang, T., Zhang, K. (2016). Chemical characterization and source apportionment of PM2.5 in a semi-arid and petrochemical-industrialized city, Northwest China. Science of the Total Environment, 573, 1031-1040.

Wang, Y., Zhuang, G., Sun, Y., An, Z., 2006. The variation of characteristics and formation mechanisms of aerosols in dust, haze, and clear days in Beijing. Atmospheric Environment 40(34), 6579-6591.

Wang, Z., Wang, T., Guo, J., Gao, R., Xue, L. K., Zhang, J. M., Zhou, Y., Zhou, X. H., Zhang, Q. Z., Wang, W. X., 2012. Formation of secondary organic carbon and cloud impact on carbonaceous aerosols at Mount Tai, North China. Atmospheric environment 46, 516-527.

Wei, F., Yang, Z., Jiang, D., Liu, Z., Sun, B., 1991. Basic statistics and features for background values of soil elements in China. Environmental Monitoring in China 7, 1-6.

WHO, 2005. World Health Organization Air Quality Guidelines Global Update, E87950.

Wu, C., Yu, J. Z., 2016. Determination of primary combustion source organic carbon-to-elemental carbon (OC/EC) ratio using ambient OC and EC measurements: secondary OC-EC correlation minimization method. Atmos. Chem. Phys., 16(8), 5453-5465.

Wu, Y., Gu, B., Erisman, J. W., Reis, S., Fang, Y., Lu, X., Zhang, X., 2016. $PM_{2.5}$ pollution is substantially affected by ammonia emissions in China. Environmental Pollution 218, 86-94.

Xiao Z., Bi X., Feng Y., Wang Y., Zhou J., Fu X., Weng, Y., 2012. Source Apportionment of Ambient PM_{10} and $PM_{2.5}$ in Urban Area of Ningbo City. Research of Environmental Sciences(China), 5, 549-555.

659 Xu, J., Tao, J., Zhang, R., Cheng, T., Leng, C., Chen, J., Huang, G., Li, X., Zhu, Z., 2012.
660 Measurements of surface aerosol optical properties in winter of Shanghai. Atmospheric research
661 109, 25-35.
662 Xu, J., Xu, H., Xiao, H., Tong, L., Snape, C., Wang, C., He, J. 2016. Aerosol composition and
663 sources during high and low pollution periods in Ningbo. Atmospheric Research. 178-179: 559-
664 569.
665 Xu, J., Xu, M., Snape, C., He, J., Behear, S., Xu, H., Ji, D., Wang, C., Yu, H., Xiao, H., Jiang, Y.,
666 Qi, B., Du, R. 2017. Temporal and spatial variation in major ion chemistry and source
667 identification of secondary inorganic aerosols in Northern Zhejiang Province, China.
668 Chemosphere. 179: 316-330.
669 Yang, L., Cheng, S., Wang, X., Nie, W., Xu, P., & Gao, X., et al. 2013. Source identification and
670 health impact of $PM_{2.5}$, in a heavily polluted urban atmosphere in china. Atmospheric
671 Environment, 75(4), 265-269.
672 Yang, Y., Liu, X., Qu, Y., Wang, J., An, J., Zhang, Y., Zhang, F., 2015. Formation mechanism of
673 continuous extreme haze episodes in the megacity Beijing, China, in January 2013. Atmospheric
674 research 155, 192-203.
675 Yao, L., Yang, L., Yuan, Q., Yan, C., Dong, C., Meng, C., et al. 2016. Sources apportionment of
676 $PM_{2.5}$, in a background site in the north china plain. Science of the Total Environment, 541, 590-8.
677 Yu J., Wang W., Zhou J., Xu D., Zhao Q., He L., 2015. Analysis of pollution characteristics and
678 sources of $PM_{2.5}$ in winter of Ningbo City. Environmental Science & Technology (China) 8, 150-
679 155.
680 Zhang, F., Wang, Z. W., Cheng, H. R., Lv, X. P., Gong, W., Wang, X. M., Zhang, G., 2015.
681 Seasonal variations and chemical characteristics of PM2.5 in Wuhan, central China. Science of the
682 Total Environment, 518, 97-105.
683 Zhang, H., Wang, S., Hao, J., Wan, L., Jiang, J., Zhang, M., et al., 2012. Chemical and size
684 characterization of particles emitted from the burning of coal and wood in rural households in
685 Guizhou, China. Atmos. Environ. 51, 94–99.

686 Zhang, Y. J., Cai, J., Wang, S., He, K. B., Zheng, M., 2017. Review of receptor-based source
687 apportionment research of fine particulate matter and its challenges in China. Science of the Total
688 Environment 586, 917–929.
689 Zhao B, Wang S, Donahue N M, Jathar, S. H., Huang, X. F., Wu, W. J., Hao, J. M., Robinson, A.
690 L., 2016. Quantifying the effect of organic aerosol aging and intermediate-volatility emissions on
691 regional-scale aerosol pollution in China. Scientific Reports 6, 28815.
692 Zhao, P., Zhang, X., Xu, X., Zhao, X., 2011. Long-term visibility trends and characteristics in the
693 region of Beijing, Tianjin, and Hebei, China. Atmospheric research 101, 711-718.

Figure legends

Fig. 1. Location of sampling site (SZ), Dongqianhu (site 1, rural site), Longsai (site 2, industrial site), Fenghua (site 3, suburban site), Wenfeng (site 4, background site), Cixi (site 5, urban), Wanli (site 6, urban site) and Beilun (site 7, industrial site) in Ningbo.

Fig. 2. Concentrations of $PM_{2.5}$ in Ningbo (a) Monthly $PM_{2.5}$ variations in urban Ningbo from 2011 to 2015 (b) Variations in $PM_{2.5}$ observed using filter sampling and automatic analyzers in this study.

Fig. 3. The regression lines of hourly $PM_{2.5}$ concentrations among multiple sites in Ningbo in this study.

Fig. 4. Chemical composition in $PM_{2.5}$ in this study **(a)** daily variation **(b)** chemical profile in $PM_{2.5}$ at various air quality levels (SP, Slightly polluted; MP, Moderately polluted; HP, Heavily polluted).

Fig. 5. The regression line between SO_2 and NO_3^- during the moderately and heavily polluted days.

Fig. 6. Correlations among inorganic ions during the sampling period, good and moderate air quality, and polluted days.

Fig. 7 (a) The relationship between the ratios of OC/EC and air pollution levels; (b) The correlation between OC/EC and EC concentration; (c) The correlation between SO_4^{2-} concentration and EC concentration; (d) The correlation between SO_4^{2-} concentration and OC concentration.

Fig. 8. Factor profile (w % of species) in each source for $PM_{2.5}$ in Ningbo.

Fig. 9. The contribution from each source to the ambient $PM_{2.5}$ in Ningbo.

Fig. 10. Backward trajectories arriving at the sampling site in Ningbo and their cluster analysis.

Fig. 11. The WPSCF maps for main chemical species and $PM_{2.5}$ in Ningbo in this study.

Fig. 12. The WCWT maps for main chemical species and $PM_{2.5}$ in Ningbo in this study.

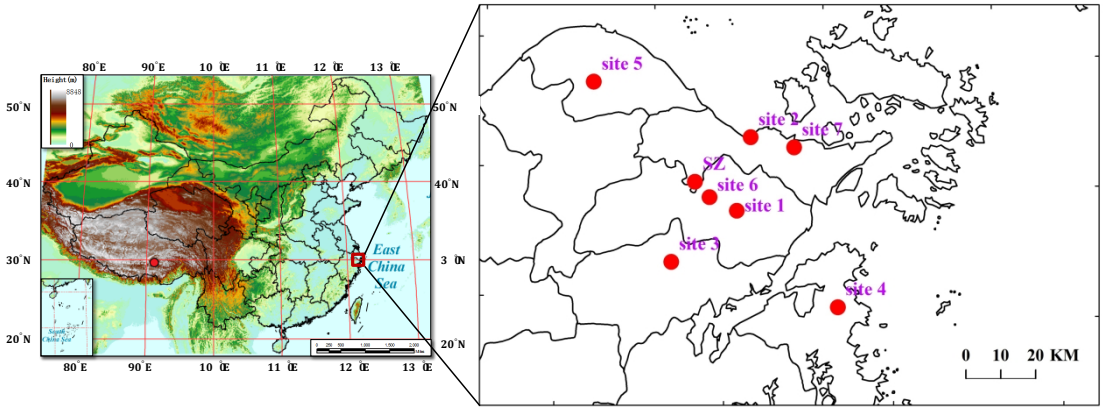

Fig. 1. Location of sampling site (SZ), Dongqianhu (site 1, rural site), Longsai (site 2, industrial site), Fenghua (site 3, suburban site), Wenfeng (site 4, background site), Cixi (site 5, urban), Wanli (site 6, urban site) and Beilun (site 7, industrial site) in Ningbo.

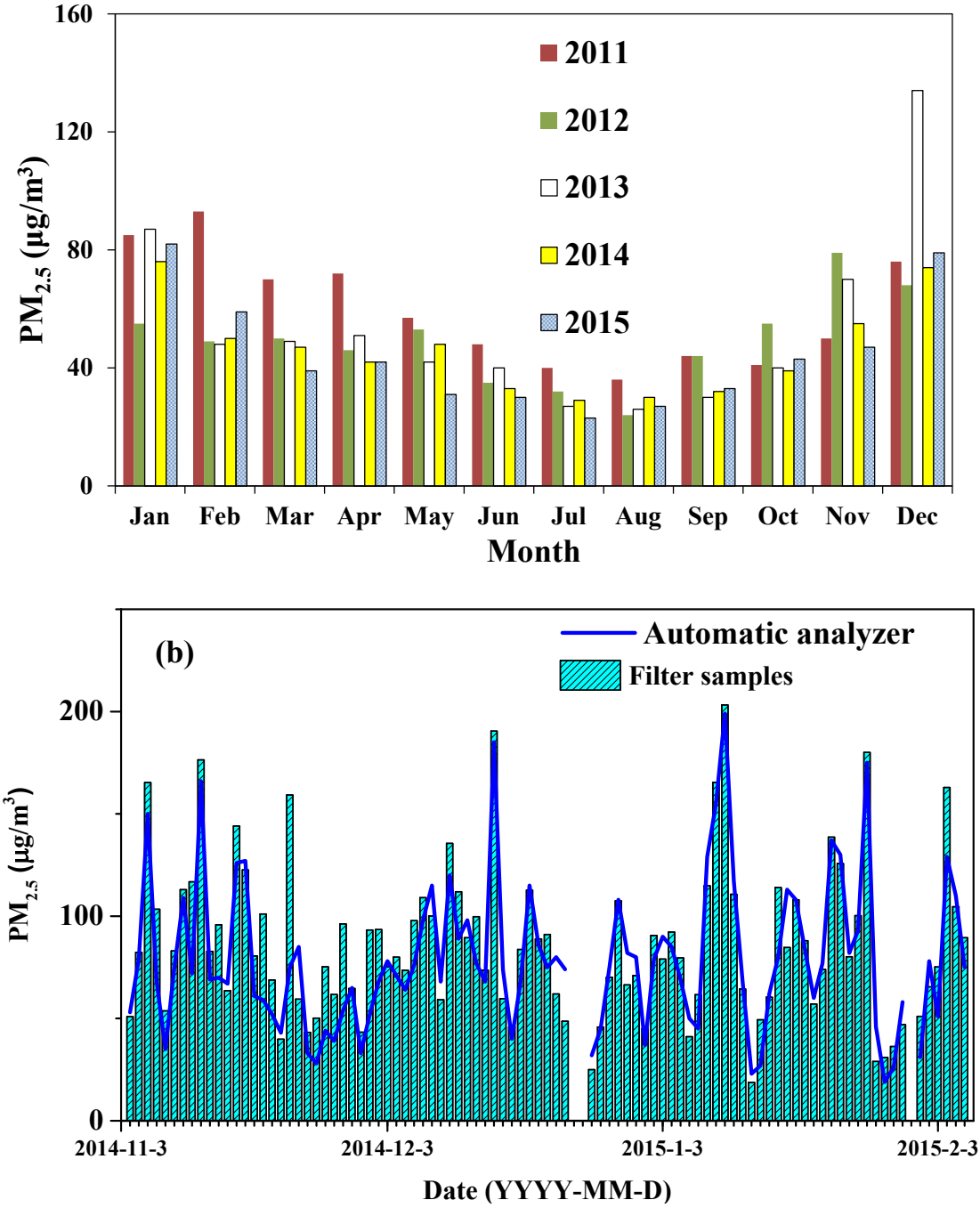

Fig. 2. $PM_{2.5}$ concentrations in Ningbo (a) Monthly $PM_{2.5}$ variations in urban Ningbo from 2011 to 2015 (b) Variations in $PM_{2.5}$ observed using filter sampling and automatic analyzers in this study.

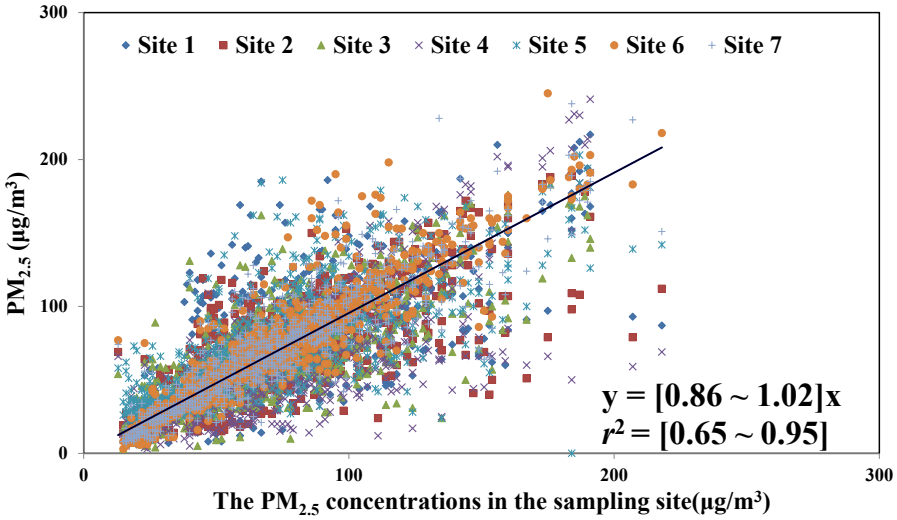

Fig. 3. The regression lines of hourly $PM_{2.5}$ concentrations among multiple sites in Ningbo in this study.

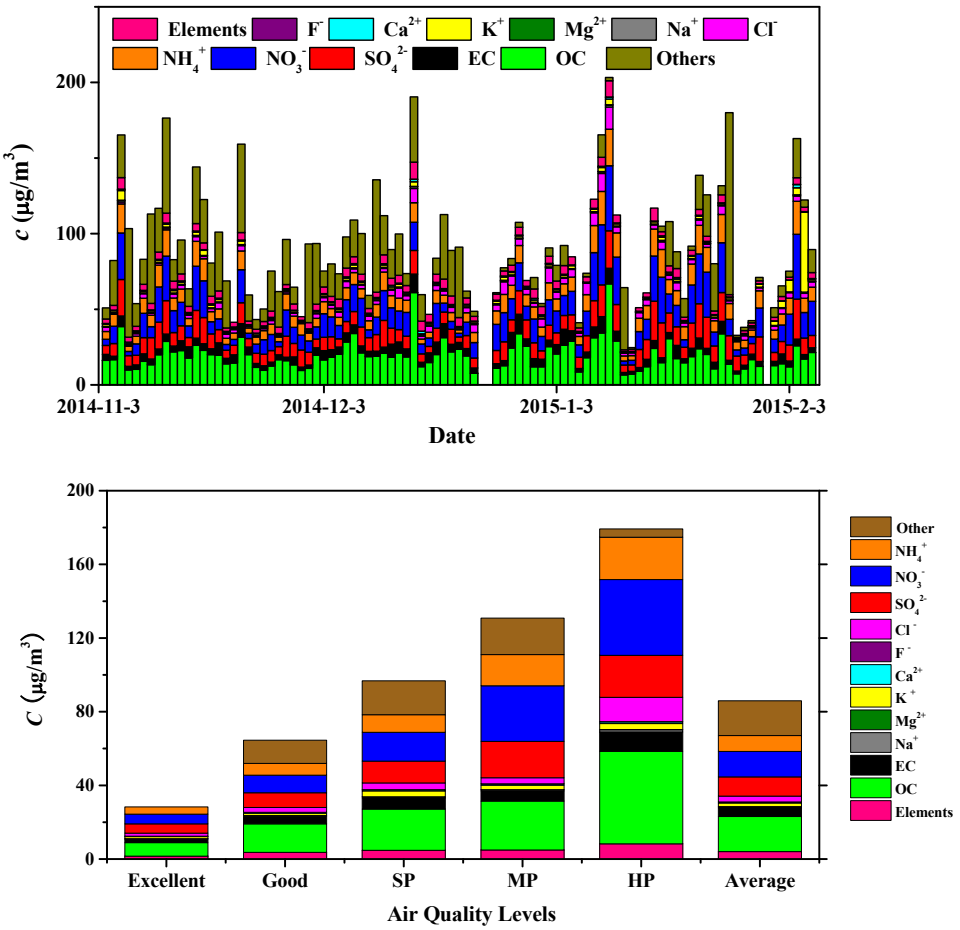

Fig. 4. Chemical composition in $PM_{2.5}$ in this study (a) daily variation (b) chemical profile in $PM_{2.5}$ at various air quality levels (SP, Slightly polluted; MP, Moderately polluted; HP, Heavily polluted).

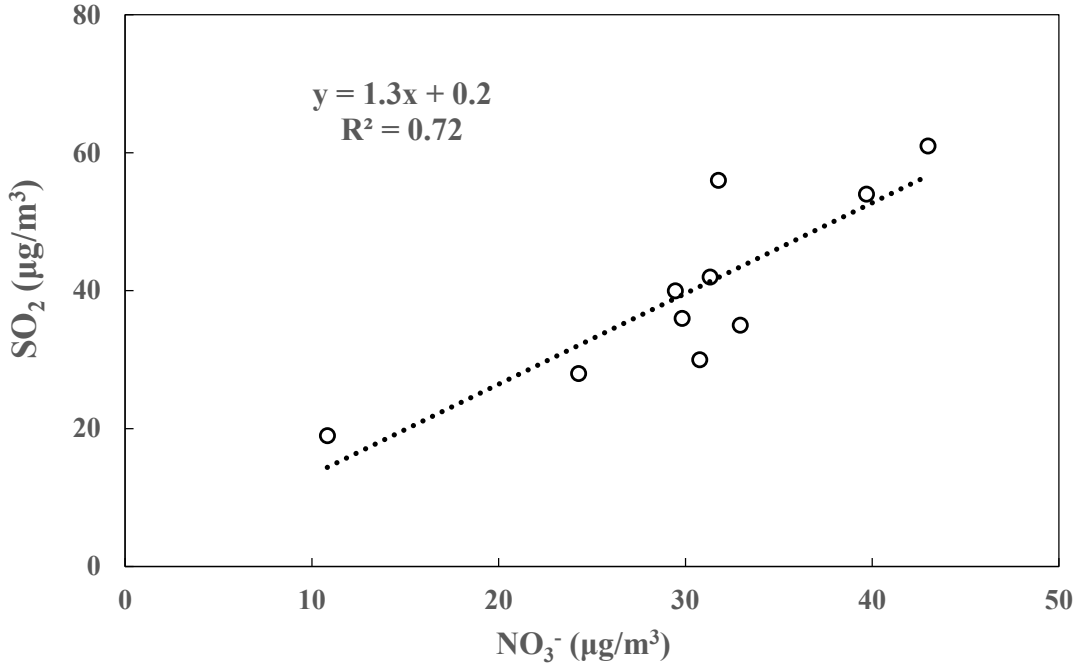

Fig. 5. The regression line between SO_2 and NO_3^- during the moderately and heavily polluted days.

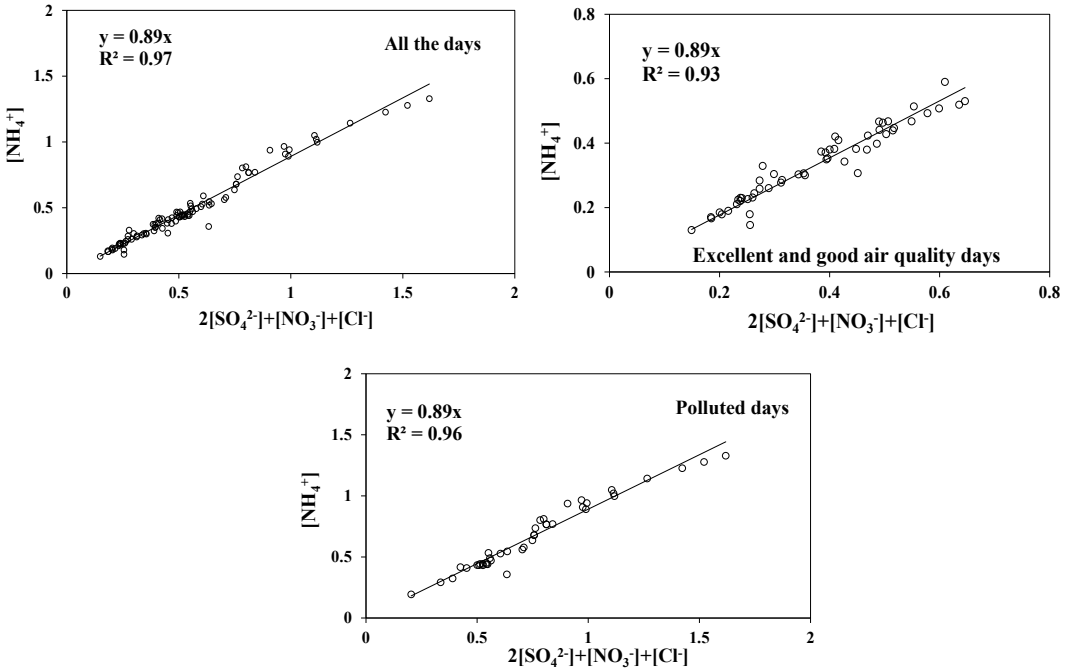

Fig. 6. Correlations among inorganic ions during the sampling period, excellent and good air quality, and polluted days.

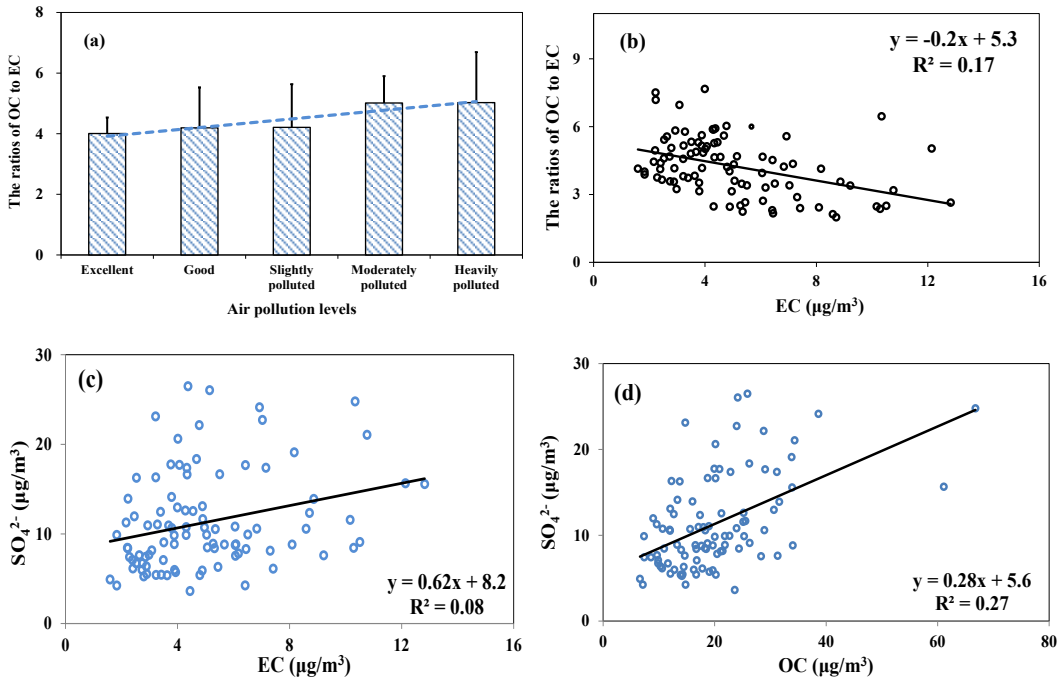

Fig. 7 (a) The relationship between the ratios of OC/EC and air pollution levels; (b) The correlation between OC/EC and EC concentration; (c) The correlation between SO_4^{2-} concentration and EC concentration;(d) The correlation between SO_4^{2-} concentration and OC concentration.

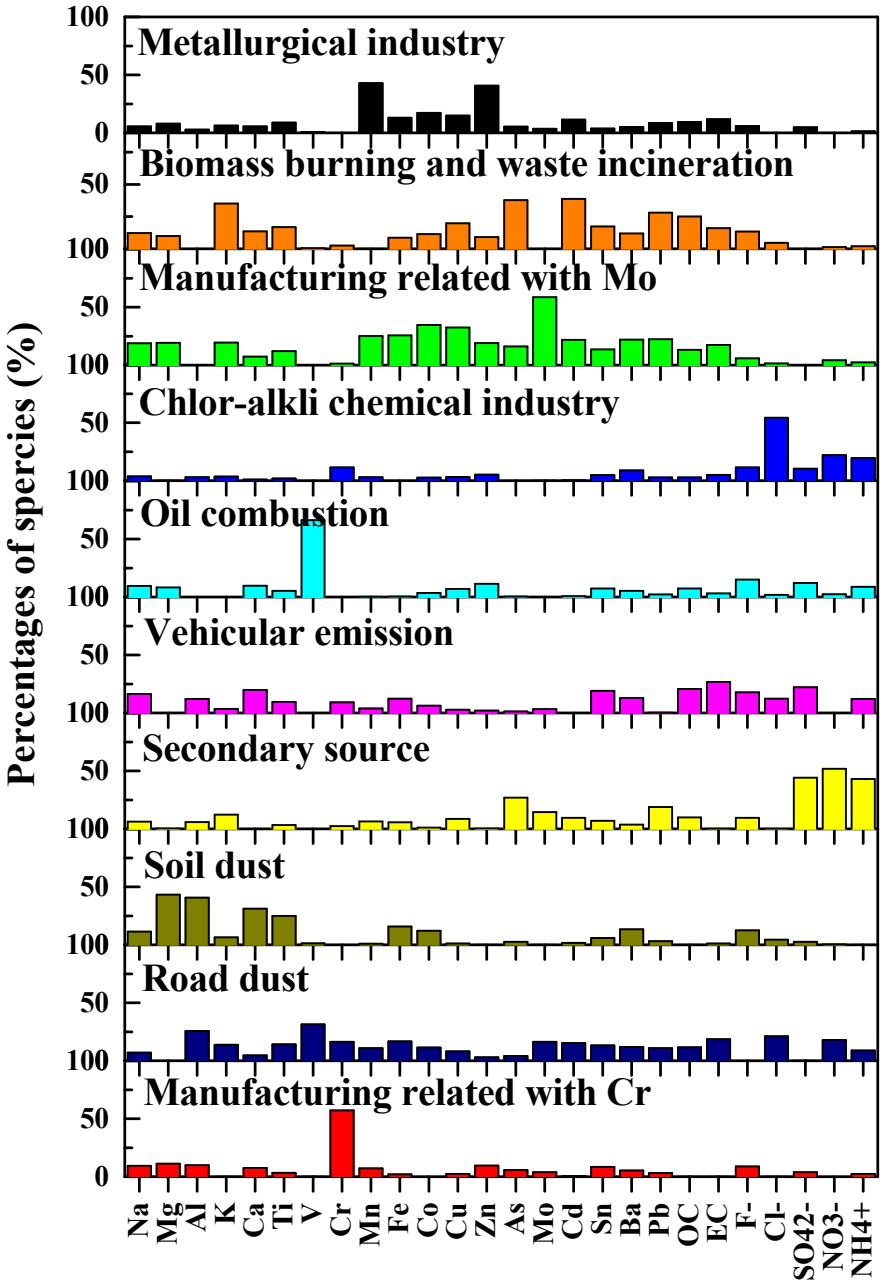

Fig. 8. Factor profile (w % of species) in each source for $PM_{2.5}$ in Ningbo.

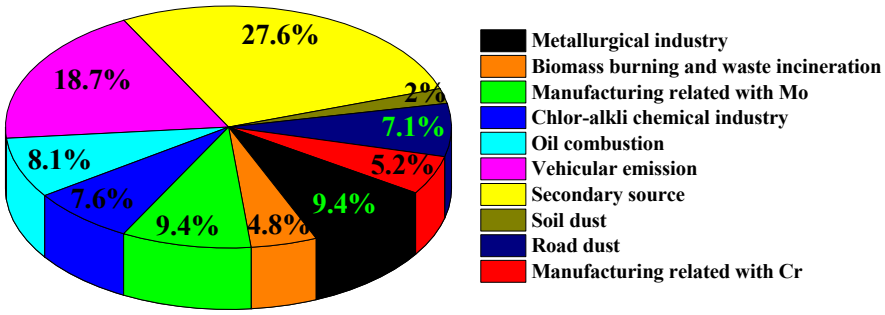

Fig. 9. The contribution from each source to the ambient $PM_{2.5}$ in Ningbo.

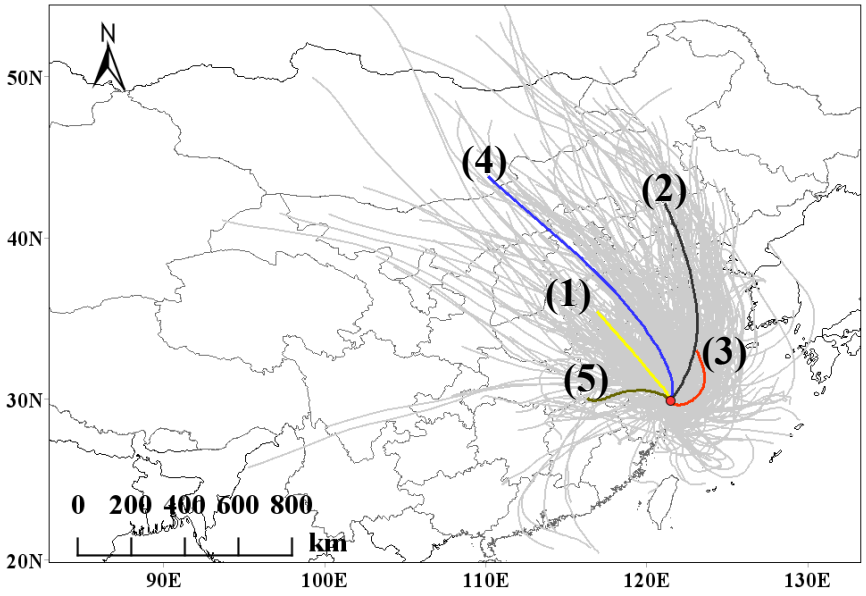

Fig. 10. Backward trajectories arriving at the sampling site in Ningbo and their cluster analysis.

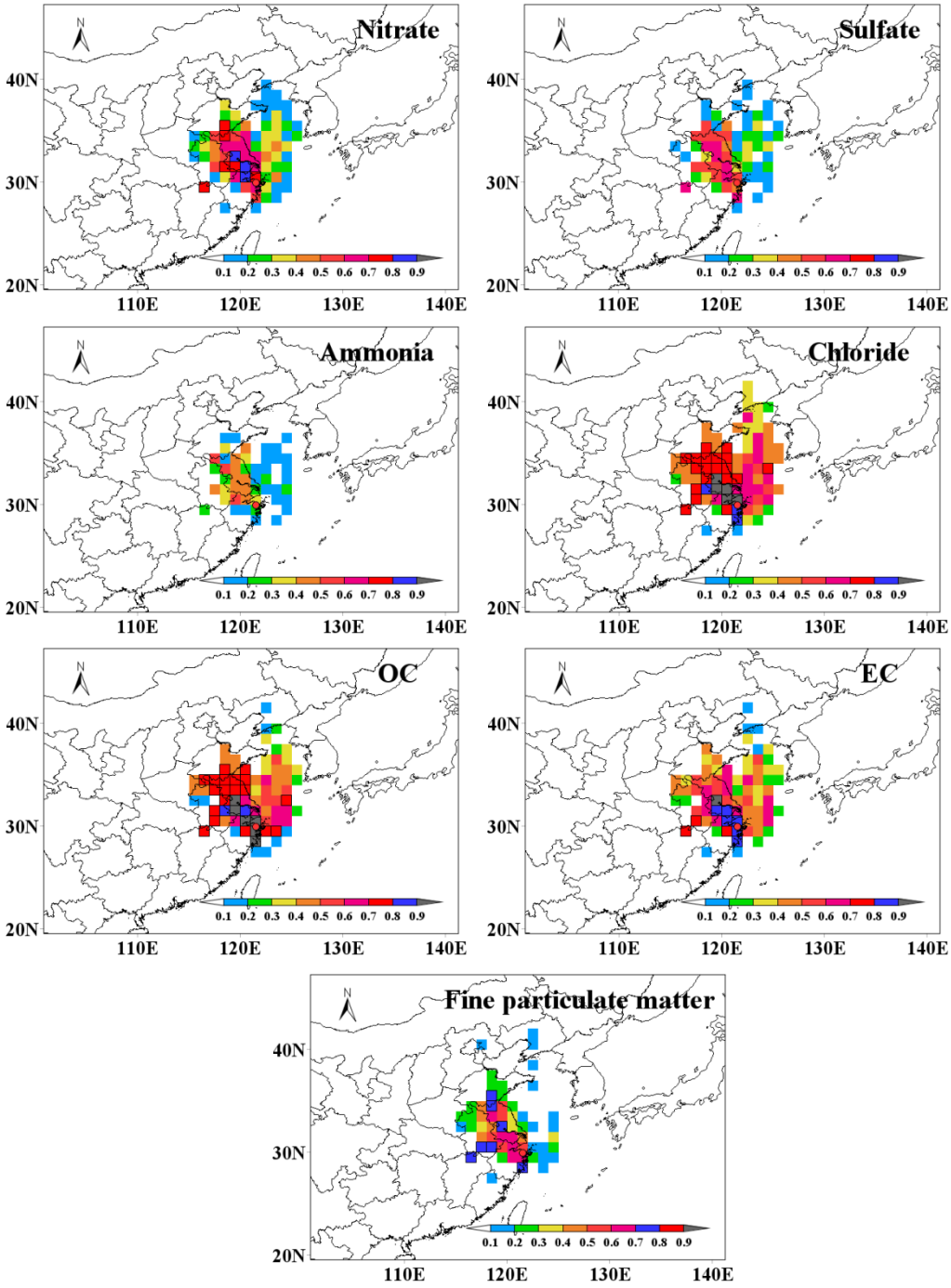

Fig. 11. The WPSCF maps for main chemical species and $PM_{2.5}$ in Ningbo in this study.

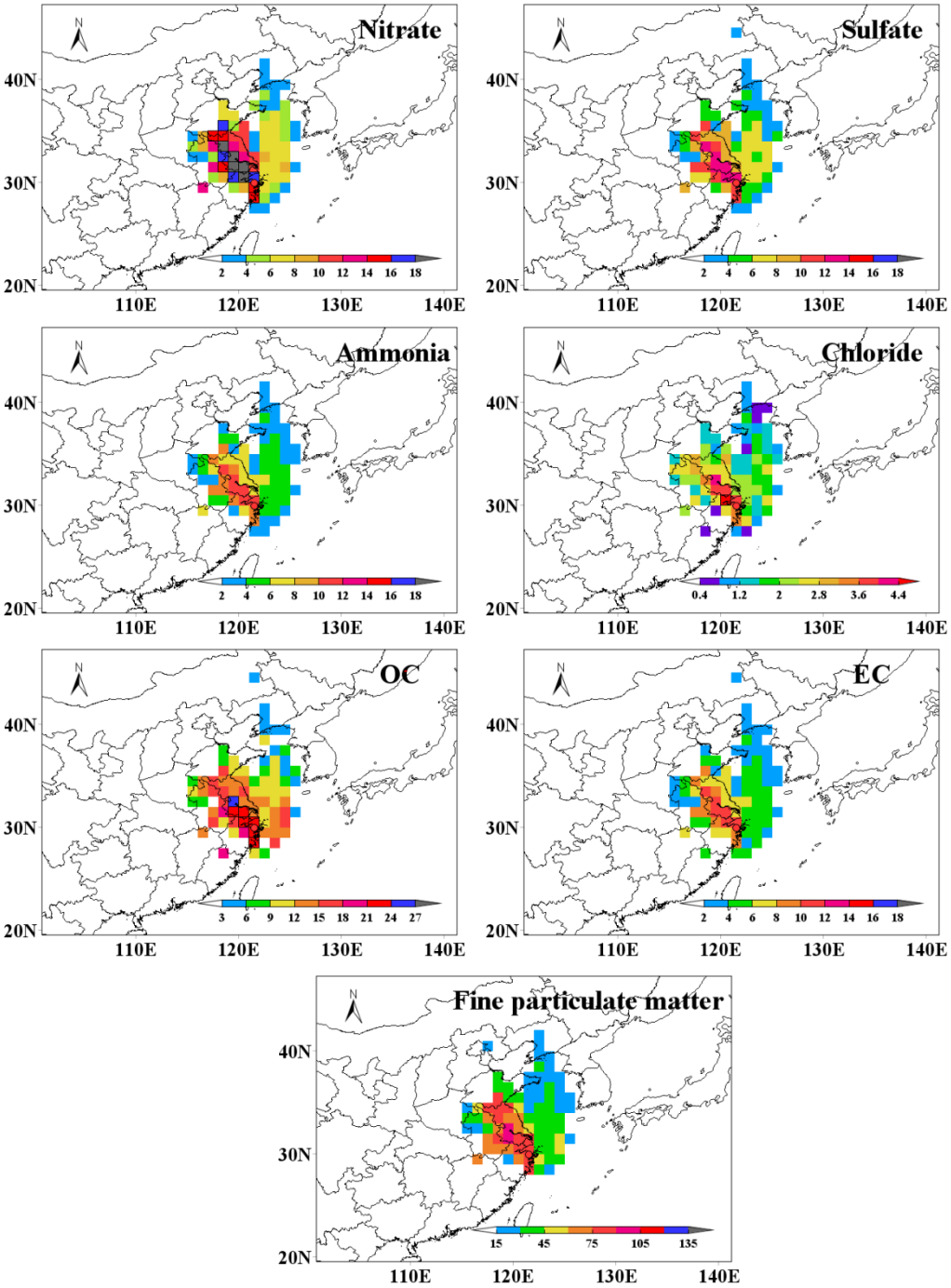

Fig. 12. The WCWT maps for main chemical species and $PM_{2.5}$ in Ningbo in this study.

Tab. 1. The average concentrations of water-soluble inorganic ions, carbonaceous species and trace elements in $PM_{2.5}$ during the sampling period (unit: $\mu g/m^3$).

Species	Mean	SD
Water-soluble inorganic ions		
SO_4^{2-}	11.2	5.4
NO_3^-	14.5	9.4
NH_4^+	9.1	4.8
Na^+	0.5	0.2
Mg^{2+}	0.1	0.0
K^+	2.0	5.3
Ca^{2+}	0.6	0.3
Cl^-	3.3	2.4
F^-	0.05	0.02
Carbonaceous species		
OC	19.0	9.8
EC	4.9	2.5
Trace elements		
Na	0.699	0.226
Mg	0.117	0.068
Al	0.616	0.614
K	1.019	0.548
Ca	0.589	0.321
Ti	0.028	0.019
V	0.006	0.005
Cr	0.029	0.013
Mn	0.057	0.037
Fe	0.534	0.273
Co	0.0004	0.0002
Ni	0.010	0.005
Cu	0.027	0.014
Zn	0.376	0.229
As	0.007	0.004
Mo	0.002	0.001
Ag	0.000	0.000
Cd	0.002	0.001
Sn	0.012	0.005
Ba	0.017	0.008
Tl	0.001	0.001
Pb	0.091	0.055

Supplementary materials for

Characteristics of fine particulate matter and its sources in an industrialized coastal city, Yangtze River Delta, China

Weifeng Wang[1], Jie Yu[1], Yang Cui[2], Jun He[3], Peng Xue[2], Wan Cao[2], Hongmei Ying[1], Wenkang Gao[2, 4], Yingchao Yan[2], Bo Hu[2, 4], Jinyuan Xin[2, 4], Lili Wang[2, 4], Zirui Liu[2, 4], Yang Sun[2, 4], Dongsheng Ji[2, 4*], Yuesi Wang[2, 4*]

[1] *Environment monitoring center of Ningbo, Ningbo 315012, China*

[2] *State Key Laboratory of Atmospheric Boundary Layer Physics and Atmospheric Chemistry, Institute of Atmospheric Physics, Chinese Academy of Sciences, Beijing 100029, China*

[3]*International Doctoral Innovation Centre, Natural Resources and Environment Research Group, Department of Chemical and Environmental Engineering, University of Nottingham Ningbo China, Ningbo, China*

[4]*Center for Excellence in Regional Atmospheric Environment, Institute of Urban Environment, Chinese Academy of Sciences, Xiamen 361021, China.*

[*]Corresponding author:

E-mail address: jds@mail.iap.ac.cn; wys@dq.cern.ac.cn

S2.1 PMF model

PMF model, an effective receptor modeling tool, has been worldwide applied for source apportionment in the field of environmental research and administration. Its goal is to resolve the matrix of measured sample data into factor contribution and source profiles, the mathematical equation can be shown in Equation (1):

$$x_{ij} = \sum_{k=1}^{p} g_{ik} f_{kj} + e_{ij} \quad (1)$$

where x_{ij} is the measured concentration of the jth species in the ith samples, p is the number of factors, g_{ik} is the contribution of the ith source to the ith sample, f_{kj} is the species profile of the k th source, e_{ij} is the residuals for each species.

Factor contribution and source profiles are derived by PMF minimizing the objective function Q (Equation (2)):

$$Q = \sum_{i=1}^{n} \sum_{j=1}^{m} \left[\frac{x_{ij} - \sum_{i=1}^{p} g_{ik} f_{kj}}{u_{ij}} \right]^2 \quad (2)$$

Where u_{ij} is the uncertainty of jth species in the ith sample. The uncertainty is calculated based on method detection limit (MDL) and determination error fraction. If the values are lower than MDL, they will be replaced by half of the MDL and the uncertainty will be set to 5/6 of MDL. If the values are higher than MDL, the uncertainty will be estimated according to the equation (3):

$$Un = \sqrt{(\text{Error Fraction} \times \text{concentration})^2 + (0.5 \times \text{MDL})^2} \quad (3)$$

According to the instrument measurement, Error Fraction values were set to 15%. The sampling data are input into US EPA's PMF 5.0 in this study. Three error uncertainty estimates and diagnostics (Displacement (DISP), Bootstrap (BS), BS-DISP) are used to assess the rationality of the results.

Factor contribution and source profiles are derived by PMF minimizing the objective function Q:

$$Q = \sum_{i=1}^{n} \sum_{j=1}^{m} \left[\frac{x_{ij} - \sum_{i=1}^{p} g_{ik} f_{kj}}{u_{ij}} \right]^2 \quad (4)$$

Where u_{ij} is the uncertainty of jth species in the ith sample. Q is a critical parameter for PMF and two versions of Q are displayed for the model runs: $Q_{(True)}$ is the goodness-of-fit parameter

calculated including all points and $Q_{(Robust)}$ is the goodness-of-fit parameter calculated excluding points that do not fit the modeled values, defined as samples of which the uncertainty-scaled residual is greater than 4. The difference between $Q_{(True)}$ and $Q_{(Robust)}$ is a measure of the impact of data points with high scaled residuals. If the ratio of $Q_{(True)}/Q_{(Robust)}$ is closer to 1, it indicates that there are not too many outliers affecting the results of PMF runs.

S2.2 HYSPLIT 4 model

The HYSPLIT_4 (HYbrid Single-Particle Lagrangian Integrated Trajectory) model (Version 4) is a complete system for computing simple trajectories to complex dispersion and deposition simulations using either puff or particle approaches. The model uses previously gridded meteorological data on one of three conformal map projections (Polar, Lambert, Mercator). Air concentration calculations associate the mass of pollutant species with the release of either puffs, particles, or a combination of both. The dispersion rate is calculated from the vertical diffusivity profile, wind shear, and horizontal deformation of the wind field. Air concentrations are calculated at a specific grid point for puffs and as cell average concentrations for particles (Draxler et al., 1998).

Assuming that the trajectory of the particle is moving with the wind field, the trajectory is the integral of the point in time and space. Position computed from average velocity linearly is interpolated at the initial position (P) and first-guess position (P'):

$$P(t+dt) = P(t) + 0.5\ [\ V(P\{t\}) + V(P'\{t+dt\})\ ]\ dt \quad (4)$$

$$P'(t+dt) = P(t) + V(P\{t\})\ dt \quad (5)$$

the integration time step is variable: $V_{max}\ dt < 0.75$.

Cluster analysis is a simple statistical method referring to multivaritions, whose purpose is to divide a data set into groups or "clusters" of similar cases or variable. The assignment of members (trajectories) to a given group (cluster) is carried out by minimizing the internal variability within the group of trajectories and maximizing the external variability between different groups based on the trajectory co-ordinates.

The clustering method is based on the spatial similarity of the airflow (speed and direction) to group a large number of trajectories. There are two clustering options with Euclidean distance and

angle distance (Draxler et al., 1999). The Euclidean distance between two backward trajectories is then given by

$$d_{12} = \sqrt{\sum_{i=1}^{n}((X_1(i) - X_2(i))^2 + ((Y_1(i) - Y_2(i))^2} \quad (6)$$

Where X_1 (Y_1) and X_2 (Y_2) refer to backward trajectories 1 and 2, respectively. The main disadvantage of using the Euclidean distance is that two backward trajectories following the same path but having different speed may be classified in two different clusters. Since the cluster analysis is to identify the trajectories in similar direction, the angle distance should be selected. The angle distance between two backward trajectories is defined as

$$d_{12} = \frac{1}{n}\sum_{i=1}^{n}\cos^{-1}(0.5\frac{A_i + B_i - C_i}{\sqrt{A_i B_i}}) \quad (7)$$

Where

$$A_i = (X_1(i) - X_0)^2 + (Y_1(i) - Y_0)^2 \quad (8)$$

$$B_i = (X_2(i) - X_0)^2 + (Y_2(i) - Y_0)^2 \quad (9)$$

$$C_i = (X_2(i) - X_1)^2 + (Y_2(i) - Y_1)^2 \quad (10)$$

The variables X_0 and Y_0 define the position of studied site. Note that $d12$ varies between 0 and π. The two extreme values occur when two trajectories are in the same and opposite direction, respectively. As defined by equations (7) to (10), $d12$ is the mean angle between the two backward trajectories, as seen from the studied site.

Reference

Draxler, R. R., & Hess, G. D. (1998). An overview of the hysplit-4 modeling system for trajectories. Australian Meteorological Magazine, 47(4), 295-308.

Draxler, R.R., 1999. HYSPLIT 4 User's Guide. NOAA Tech. Memo. ERL ARL-230, 35 pp. [2016 version available online at: http://www.arl.noaa.gov/documents/reports/hysplit_user_guide.pdf. last access: January 2016].

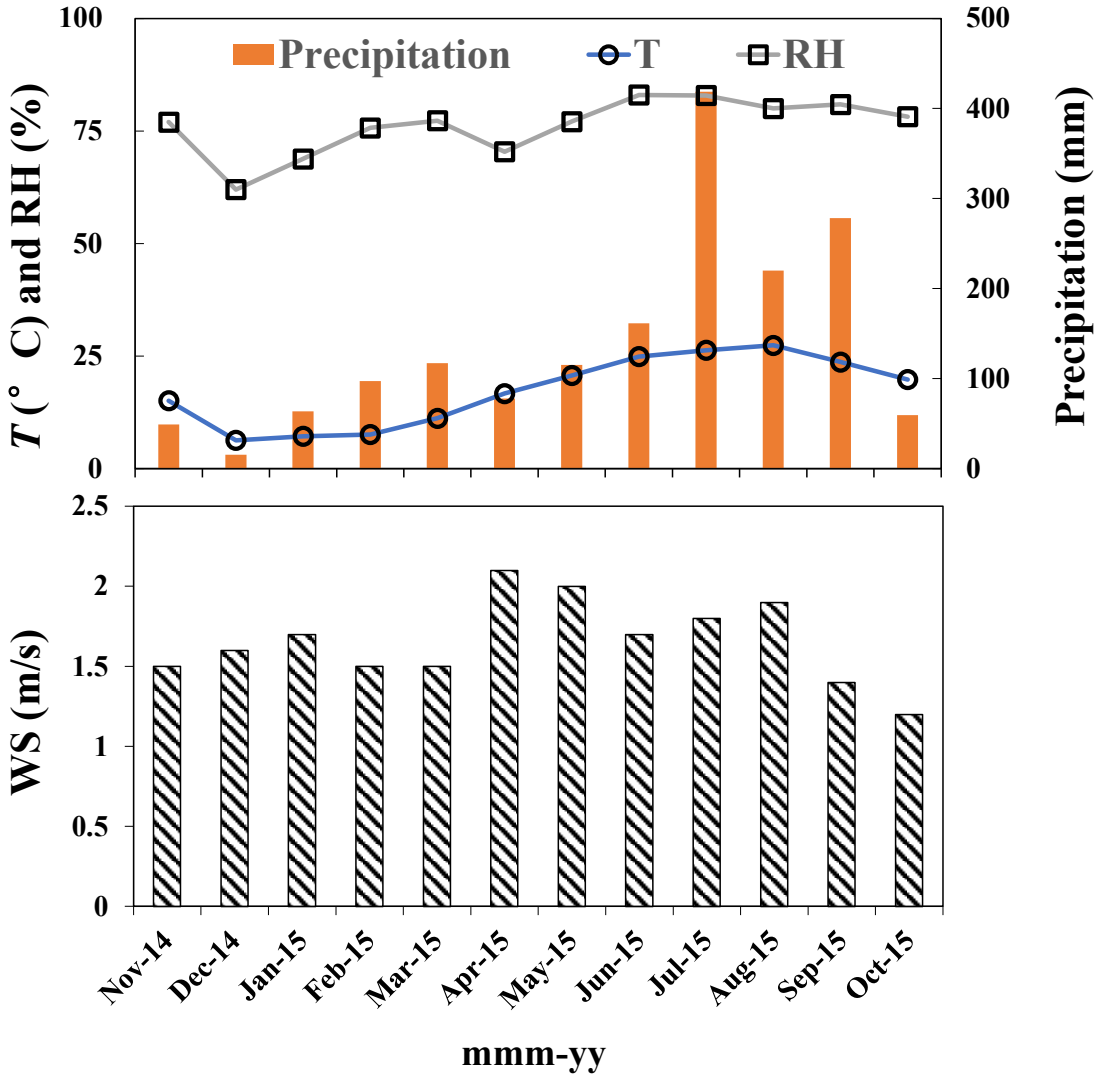

Fig. S1. Monthly variations in the meteorological parameters (Precipitation, RH, T and WS).

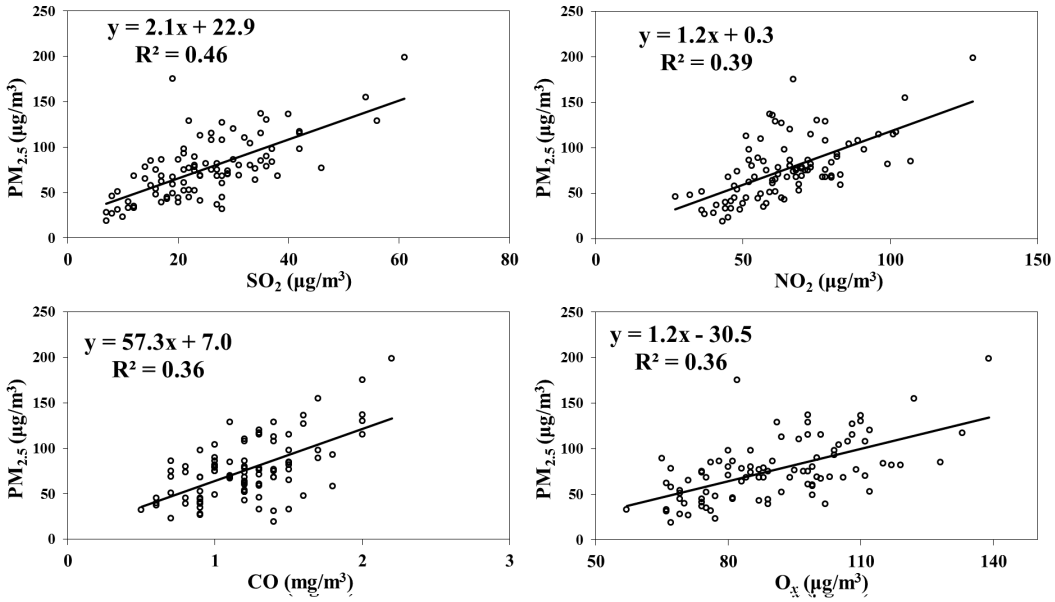

Fig. S2. The regression lines between SO_2, NO_2, CO and O_x and $PM_{2.5}$ during the sampling period.

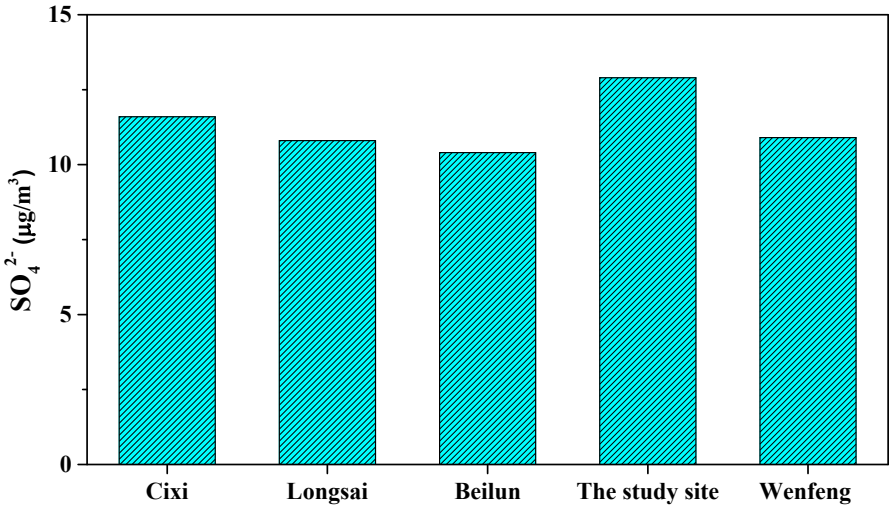

Fig. S3. Spatial distribution of SO_4^{2-} at Cixi, Longsai, Beilun, the study and Wenfeng sites in Ningbo (Data cited from the report of source apportionment in Ningbo).

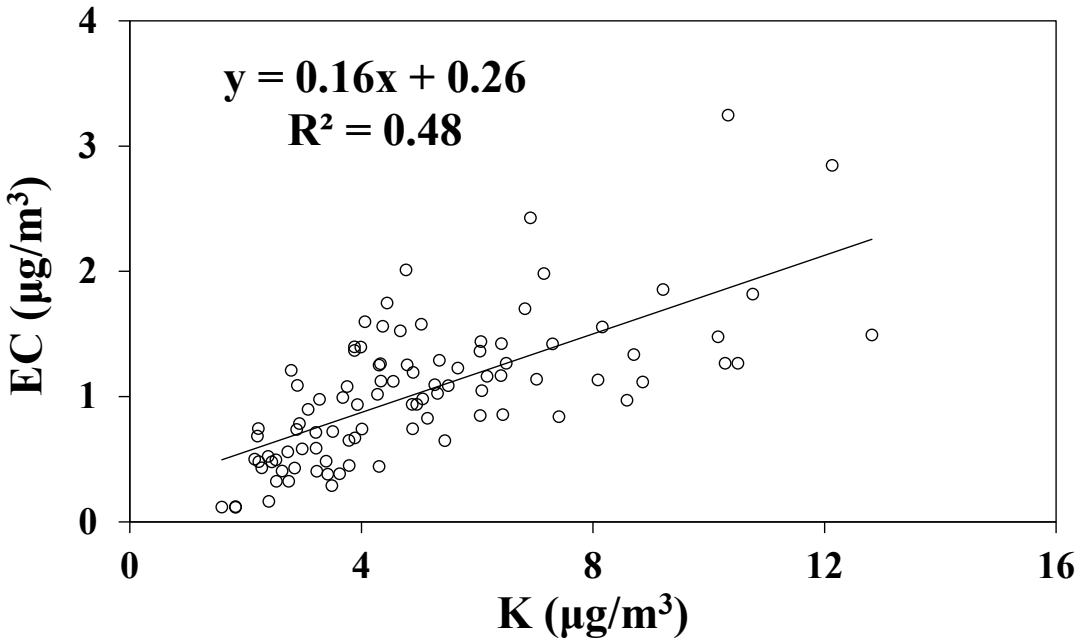

Fig. S4. The regression lines between EC and K during the sampling period.

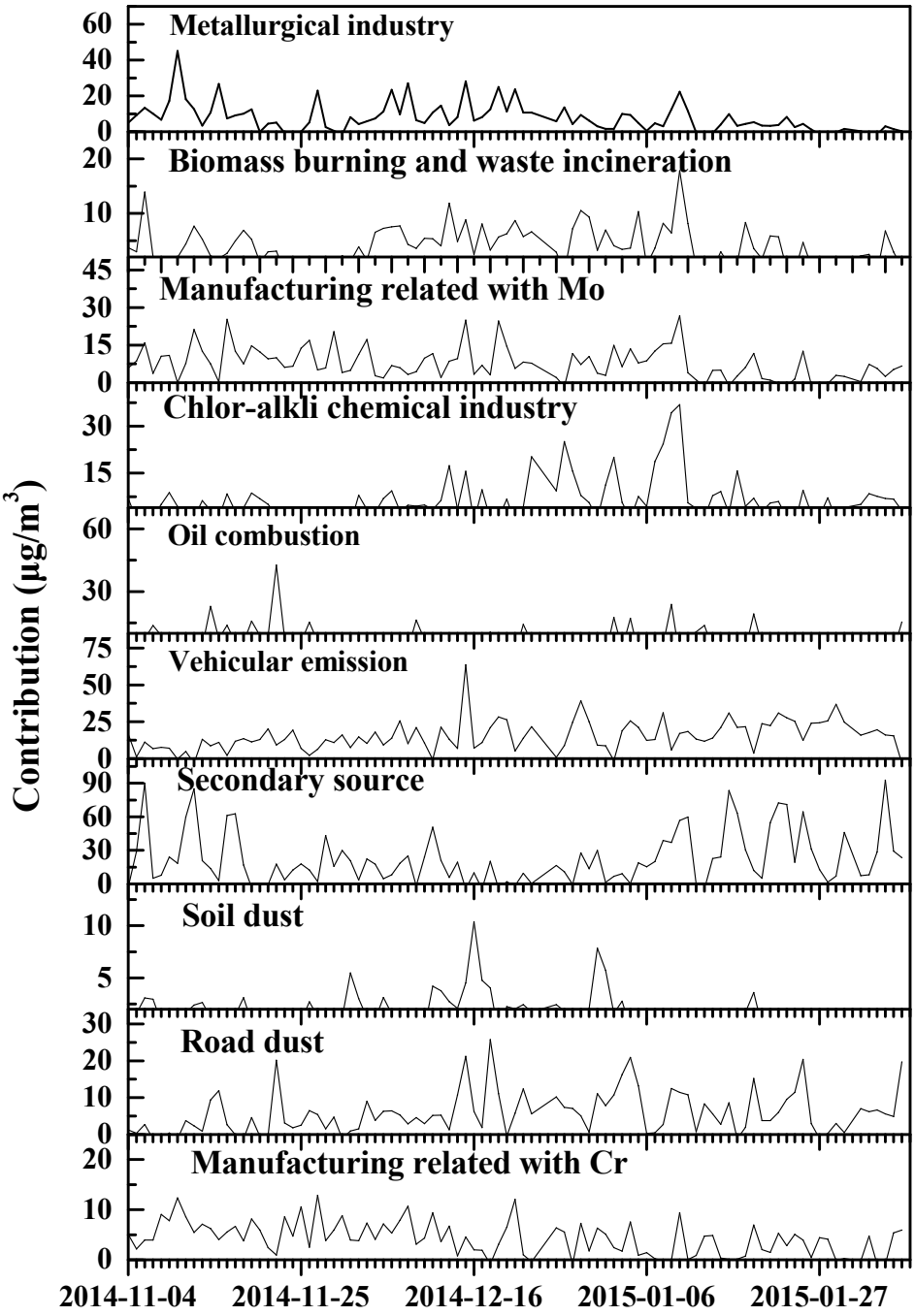

Fig. S5. Daily contribution of each source obtained by PMF analysis.

Tab. S1 The categorization of air quality levels based on $PM_{2.5}$ concentration bands and the numbers of days with different air quality levels during the sampling period.

Air quality levels	Excellent	Good	SP	MP	HP
Data intervals of daily $PM_{2.5}$ concentrations ($\mu g/m^3$)	0-35	35-75	75-115	115-150	150-250
The numbers of days	2	48	31	8	3

Tab. S2. Inventory of air pollutants from anthropogenic emission In Ningbo (Unit: $\times 10^4$ ton each year).

Category	SO_2	NO_x	CO	NH_3	VOCs
Power plant	8.85	25.33	9.32	0.00	0.63
Industrial combustion	3.45	1.75	1.97	0.00	0.57
Industrial process	4.56	1.55	5.28	0.12	10.84
Residential source	0.07	0.17	6.72	0.02	2.32
Agricultural source	0.01	0.10	1.81	1.97	0.81
Storage and transportation of oil and gas	0.00	0.00	0.00	0.00	0.57
Mobile source	0.14	4.11	14.97	0.00	2.62
Ship emission	1.79	2.50	0.05	0.00	0.06
Other anthropogenic emission	0.08	1.60	0.78	0.11	0.21

Tab. S3. Correlations between fine particulate matter ($PM_{2.5}$) and elements during the sampling period.

		$PM_{2.5}$	Na	Mg	Al	K	Ca	Ti	V	Cr	Mn	Fe	Co	Ni	Cu	Zn	As	Mo	Ag	Cd	Sn	Ba	Tl	Pb
PM_{25}	Pearson Correlation	1.00	0.51	0.16	0.06	0.61	0.27	0.20	0.07	0.17	0.43	0.51	0.37	0.14	0.40	0.31	0.60	0.52	0.50	0.58	0.52	0.45	0.26	0.65
	Sig. (2-tailed)		0.0000	0.1376	0.5457	0.0000	0.0085	0.0598	0.4943	0.0970	0.0000	0.0000	0.0003	0.1905	0.0001	0.0022	0.0000	0.0000	0.0000	0.0000	0.0000	0.0000	0.0127	0.0000
Na	Pearson Correlation	0.51	1.00	0.63	0.18	0.91	0.58	0.42	0.25	0.45	0.73	0.89	0.86	0.46	0.76	0.66	0.67	0.79	0.60	0.83	0.77	0.83	0.26	0.79
	Sig. (2-tailed)	0.0000		0.0000	0.0773	0.0000	0.0000	0.0000	0.0111	0.0000	0.0000	0.0000	0.0000	0.0000	0.0000	0.0000	0.0000	0.0000	0.0000	0.0000	0.0000	0.0000	0.0084	0.0000
Mg	Pearson Correlation	0.16	0.63	1.00	0.32	0.56	0.89	0.48	0.07	0.27	0.45	0.69	0.63	0.23	0.41	0.38	0.38	0.37	0.30	0.44	0.36	0.55	0.15	0.42
	Sig. (2-tailed)	0.1376	0.0000		0.0011	0.0000	0.0000	0.0000	0.4974	0.0065	0.0000	0.0000	0.0000	0.0225	0.0000	0.0001	0.0001	0.0001	0.0028	0.0000	0.0002	0.0000	0.1480	0.0000
Al	Pearson Correlation	0.06	0.18	0.32	1.00	0.21	0.36	0.15	(0.02)	0.05	0.21	0.28	0.19	0.09	0.13	0.04	0.23	0.07	0.10	0.15	0.20	0.17	(0.00)	0.15
	Sig. (2-tailed)	0.5457	0.0773	0.0011		0.0366	0.0002	0.1414	0.8315	0.6387	0.0368	0.0046	0.0556	0.3539	0.2089	0.7227	0.0214	0.4782	0.3194	0.1286	0.0472	0.0838	0.9782	0.1303
K	Pearson Correlation	0.61	0.91	0.56	0.21	1.00	0.56	0.41	0.13	0.38	0.73	0.88	0.83	0.38	0.76	0.62	0.82	0.77	0.71	0.91	0.81	0.82	0.31	0.89
	Sig. (2-tailed)	0.0000	0.0000	0.0000	0.0366		0.0000	0.0000	0.2025	0.0001	0.0000	0.0000	0.0000	0.0001	0.0000	0.0000	0.0000	0.0000	0.0000	0.0000	0.0000	0.0000	0.0019	0.0000
Ca	Pearson Correlation	0.27	0.58	0.89	0.36	0.56	1.00	0.50	0.03	0.17	0.38	0.68	0.57	0.16	0.32	0.28	0.36	0.30	0.27	0.44	0.40	0.52	0.14	0.38
	Sig. (2-tailed)	0.0085	0.0000	0.0000	0.0002	0.0000		0.0000	0.7646	0.0876	0.0001	0.0000	0.0000	0.1019	0.0012	0.0049	0.0003	0.0028	0.0075	0.0000	0.0000	0.0000	0.1606	0.0001
Ti	Pearson Correlation	0.20	0.42	0.48	0.15	0.41	0.50	1.00	0.11	0.22	0.49	0.51	0.46	0.27	0.36	0.50	0.30	0.26	0.25	0.40	0.36	0.35	0.09	0.39
	Sig. (2-tailed)	0.0598	0.0000	0.0000	0.1414	0.0000	0.0000		0.2762	0.0295	0.0000	0.0000	0.0000	0.0059	0.0003	0.0000	0.0021	0.0083	0.0121	0.0000	0.0003	0.0003	0.3554	0.0001
V	Pearson Correlation	0.07	0.25	0.07	(0.02)	0.13	0.03	0.11	1.00	0.09	0.16	0.17	0.27	0.33	0.19	0.26	(0.03)	0.32	0.02	0.18	0.20	0.21	(0.06)	0.13
	Sig. (2-tailed)	0.4943	0.0111	0.4974	0.8315	0.2025	0.7646	0.2762		0.3671	0.1082	0.0933	0.0057	0.0007	0.0644	0.0083	0.7313	0.0010	0.8541	0.0722	0.0423	0.0385	0.5407	0.1951
Cr	Pearson Correlation	0.17	0.45	0.27	0.05	0.38	0.17	0.22	0.09	1.00	0.57	0.48	0.39	0.34	0.40	0.51	0.27	0.39	0.21	0.37	0.36	0.37	0.07	0.40
	Sig. (2-tailed)	0.0970	0.0000	0.0065	0.6387	0.0001	0.0876	0.0295	0.3671		0.0000	0.0000	0.0001	0.0006	0.0000	0.0000	0.0074	0.0001	0.0384	0.0001	0.0003	0.0002	0.4944	0.0000
Mn	Pearson Correlation	0.43	0.73	0.45	0.21	0.73	0.38	0.49	0.16	0.57	1.00	0.77	0.74	0.45	0.65	0.86	0.60	0.67	0.50	0.72	0.60	0.62	0.20	0.74
	Sig. (2-tailed)	0.0000	0.0000	0.0000	0.0368	0.0000	0.0001	0.0000	0.1082	0.0000		0.0000	0.0000	0.0000	0.0000	0.0000	0.0000	0.0000	0.0000	0.0000	0.0000	0.0000	0.0442	0.0000
Fe	Pearson Correlation	0.51	0.89	0.69	0.28	0.88	0.68	0.51	0.17	0.48	0.77	1.00	0.84	0.39	0.67	0.62	0.65	0.76	0.54	0.82	0.77	0.82	0.25	0.80
	Sig. (2-tailed)	0.0000	0.0000	0.0000	0.0046	0.0000	0.0000	0.0000	0.0933	0.0000	0.0000		0.0000	0.0000	0.0000	0.0000	0.0000	0.0000	0.0000	0.0000	0.0000	0.0000	0.0132	0.0000
Co	Pearson Correlation	0.37	0.86	0.63	0.19	0.83	0.57	0.46	0.27	0.39	0.74	0.84	1.00	0.58	0.72	0.68	0.63	0.73	0.52	0.75	0.70	0.75	0.27	0.70
	Sig. (2-tailed)	0.0003	0.0000	0.0000	0.0556	0.0000	0.0000	0.0000	0.0057	0.0001	0.0000	0.0000		0.0000	0.0000	0.0000	0.0000	0.0000	0.0000	0.0000	0.0000	0.0000	0.0063	0.0000
Ni	Pearson Correlation	0.14	0.46	0.23	0.09	0.38	0.16	0.27	0.33	0.34	0.45	0.39	0.58	1.00	0.32	0.50	0.21	0.33	0.15	0.37	0.42	0.36	0.15	0.26
	Sig. (2-tailed)	0.1905	0.0000	0.0225	0.3539	0.0001	0.1019	0.0059	0.0007	0.0006	0.0000	0.0000	0.0000		0.0014	0.0000	0.0358	0.0008	0.1304	0.0002	0.0000	0.0003	0.1310	0.0104
Cu	Pearson Correlation	0.40	0.76	0.41	0.13	0.76	0.32	0.36	0.19	0.40	0.65	0.67	0.72	0.32	1.00	0.61	0.64	0.68	0.52	0.76	0.74	0.65	0.21	0.74
	Sig. (2-tailed)	0.0001	0.0000	0.0000	0.2089	0.0000	0.0012	0.0003	0.0644	0.0000	0.0000	0.0000	0.0000	0.0014		0.0000	0.0000	0.0000	0.0000	0.0000	0.0000	0.0000	0.0350	0.0000
Zn	Pearson Correlation	0.31	0.66	0.38	0.04	0.62	0.28	0.50	0.26	0.51	0.86	0.62	0.68	0.50	0.61	1.00	0.48	0.55	0.37	0.65	0.51	0.51	0.19	0.62
	Sig. (2-tailed)	0.0022	0.0000	0.0001	0.7227	0.0000	0.0049	0.0000	0.0083	0.0000	0.0000	0.0000	0.0000	0.0000	0.0000		0.0000	0.0000	0.0001	0.0000	0.0000	0.0000	0.0547	0.0000
As	Pearson Correlation	0.60	0.67	0.38	0.23	0.82	0.36	0.30	(0.03)	0.27	0.60	0.65	0.63	0.21	0.64	0.48	1.00	0.66	0.73	0.80	0.61	0.58	0.36	0.84
	Sig. (2-tailed)	0.0000	0.0000	0.0001	0.0214	0.0000	0.0003	0.0021	0.7313	0.0074	0.0000	0.0000	0.0000	0.0358	0.0000	0.0000		0.0000	0.0000	0.0000	0.0000	0.0000	0.0003	0.0000
Mo	Pearson Correlation	0.52	0.79	0.37	0.07	0.77	0.30	0.26	0.32	0.39	0.67	0.76	0.73	0.33	0.68	0.55	0.66	1.00	0.52	0.76	0.66	0.75	0.25	0.80
	Sig. (2-tailed)	0.0000	0.0000	0.0001	0.4782	0.0000	0.0028	0.0083	0.0010	0.0001	0.0000	0.0000	0.0000	0.0008	0.0000	0.0000	0.0000		0.0000	0.0000	0.0000	0.0000	0.0125	0.0000
Ag	Pearson Correlation	0.50	0.60	0.30	0.10	0.71	0.27	0.25	0.02	0.21	0.50	0.54	0.52	0.15	0.52	0.37	0.73	0.52	1.00	0.65	0.55	0.59	0.19	0.70
	Sig. (2-tailed)	0.0000	0.0000	0.0028	0.3194	0.0000	0.0075	0.0121	0.8541	0.0384	0.0000	0.0000	0.0000	0.1304	0.0000	0.0001	0.0000	0.0000		0.0000	0.0000	0.0000	0.0639	0.0000
Cd	Pearson Correlation	0.58	0.83	0.44	0.15	0.91	0.44	0.40	0.18	0.37	0.72	0.82	0.75	0.37	0.76	0.65	0.80	0.76	0.65	1.00	0.80	0.76	0.33	0.90
	Sig. (2-tailed)	0.0000	0.0000	0.0000	0.1286	0.0000	0.0000	0.0000	0.0722	0.0001	0.0000	0.0000	0.0000	0.0002	0.0000	0.0000	0.0000	0.0000	0.0000		0.0000	0.0000	0.0008	0.0000
Sn	Pearson Correlation	0.52	0.77	0.36	0.20	0.81	0.40	0.36	0.20	0.36	0.60	0.77	0.70	0.42	0.74	0.51	0.61	0.66	0.55	0.80	1.00	0.69	0.32	0.74
	Sig. (2-tailed)	0.0000	0.0000	0.0002	0.0472	0.0000	0.0000	0.0003	0.0423	0.0003	0.0000	0.0000	0.0000	0.0000	0.0000	0.0000	0.0000	0.0000	0.0000	0.0000		0.0000	0.0011	0.0000
Ba	Pearson Correlation	0.45	0.83	0.55	0.17	0.82	0.52	0.35	0.21	0.37	0.62	0.82	0.75	0.36	0.65	0.51	0.58	0.75	0.59	0.76	0.69	1.00	0.14	0.74
	Sig. (2-tailed)	0.0000	0.0000	0.0000	0.0838	0.0000	0.0000	0.0003	0.0385	0.0002	0.0000	0.0000	0.0000	0.0003	0.0000	0.0000	0.0000	0.0000	0.0000	0.0000	0.0000		0.1506	0.0000
Tl	Pearson Correlation	0.26	0.26	0.15	(0.00)	0.31	0.14	0.09	(0.06)	0.07	0.20	0.25	0.27	0.15	0.21	0.19	0.36	0.25	0.19	0.33	0.32	0.14	1.00	0.26
	Sig. (2-tailed)	0.0127	0.0084	0.1480	0.9782	0.0019	0.1606	0.3554	0.5407	0.4944	0.0442	0.0132	0.0063	0.1310	0.0350	0.0547	0.0003	0.0125	0.0639	0.0008	0.0011	0.1506		0.0080
Pb	Pearson Correlation	0.65	0.79	0.42	0.15	0.89	0.38	0.39	0.13	0.40	0.74	0.80	0.70	0.26	0.74	0.62	0.84	0.80	0.70	0.90	0.74	0.74	0.26	1.00
	Sig. (2-tailed)	0.0000	0.0000	0.0000	0.1303	0.0000	0.0001	0.0001	0.1951	0.0000	0.0000	0.0000	0.0000	0.0104	0.0000	0.0000	0.0000	0.0000	0.0000	0.0000	0.0000	0.0000	0.0080	

Tab. S4. Summary of PMF and EE diagnostics by run in the PMF model operation.

Diagnostic	5 factors	6 factors	7 factors	8 factors	9 factors	10 factors	11 factors	12 factors	13 factors
Q_{exp}	1906	1788	1670	1552	1434	1316	1198	1080	962
$Q_{(True)}$	9803.7	8026.3	6264.2	5299.6	4394.7	3731.3	3160.6	2645.0	2316.7
$Q_{(Robust)}$	8990.3	7360.9	5772.6	4937.7	4130.7	3475.5	2939.5	2475.8	2109.3
$Q_{(Robust)}/Q_{exp}$	4.7	4.1	3.5	3.2	2.9	2.6	2.5	2.3	2.2
DISP %dQ	<0.1%	<0.1%	<0.1%	<0.1%	<0.1%	<0.1%	<0.1%	<0.1%	<0.1%
DISP swaps	0	0	0	0	0	0	0	0	0
Factors with BS					1st F:84%		2nd F:94%	1st F:61%	5th F:84%
mapping <100%					4th F:62%		7th F:66%	2nd F:84%	8th F: 65%
					6th F:91%		10th F:68%	11th F: 67%	10th F:77%
							11th F:98%		
BS-DISP % cases with swaps	0%	0%	0%	0%	0%	0%	23%	34%	19%

F represents Factor

Tab. S5. The association of the backward trajectories with $PM_{2.5}$ concentrations.

Cluster	Average	STDEV
(1)	89.0	53.0
(2)	74.5	47.6
(3)	70.0	48.3
(4)	81.1	40.2
(5)	84.1	37.6